apoptosis, and signal transduction were enriched in DAC-treated cells, as compared to mock-treated cells.

## Expression analysis of genes identified by microarray

Database analysis revealed that out of 288 genes upregulated by DAC, 155 contain CpG islands in the 5′ end of the gene (Supplementary Table 3). We next selected ten genes known from earlier work to be cancer-related and to have CpG islands in their 5′ ends (Fig. 1). The selected genes were DFNA5, SFRP1, DKK3, PGP9.5, and LOXL4, which were all previously shown to be silenced by DNA methylation in various types of tumors [26–30]; NTN4, which encodes a member of the netrin family involved in the negative regulation of angiogenesis [31]; TRIM50, which encodes an E3 ubiquitin ligase [32]; FKBP6, which encodes an immunophilin family protein [33]; PON1, which encodes an arylesterase and whose polymorphisms are known to be associated with prostate cancer [34]; and OSBPL3, which encodes an oxysterol-binding protein that plays a role in cell adhesion [35]. Real-time PCR analysis revealed that the expression levels of all these genes were low or negligible in MCF7 cells, whereas high levels of expression—i.e., an expression ratio against GAPDH $>0.01$—were detected for DFNA5, SFRP1, OSBPL3, NTN4, PGP9.5, and LOXL4 in normal breast tissue; cell lines other than MCF7 showed various levels of expression (Supplementary Fig. 2). For DKK3, FKBP6, PON1, and TRIM50, expression was low—i.e., an expression ratio against GAPDH $< 0.01$—in normal breast tissue, and cell lines showed various levels of expression (Supplementary Fig. 3). Treatment with DAC restored expression of these genes in cell lines in which expression was otherwise low or negligible (Supplementary Fig. 3).

## Methylation analysis of ten genes in breast cancer cell lines

To confirm methylation-dependent gene silencing, we next used bisulfite-pyrosequencing to examine the methylation status of the ten genes. This enabled us to quantify the methylation of multiple CpG sites (Fig. 2). The primers and probes were designed to detect methylation in the region around the transcription start sites. Dense methylation of nine genes (SFRP1, DFNA5, DKK3, PGP9.5, OSBPL3, NTN4, TRIM50, FKBP6, and PON1) was detected in MCF7 cells, strongly suggesting that DNA methylation is the cause of gene silencing. Various levels of methylation were detected in four other cell lines and was also associated with gene silencing (Figs. 1, 2; Supplementary Figs. 2, 3). That methylation of LOXL4 was not detected means that LOXL4 is silenced by a mechanism other than DNA methylation.

**Fig. 1** Real-time PCR analysis of genes upregulated by DAC. The expression status of DFNA5, SFRP1, DKK3, FKBP6, LOXL4, OSBPL3, NTN4, PGP9.5, PON1, and TRIM50 was confirmed by real-time PCR. The cell lines and tissues examined are shown below the columns. Cell lines were treated for 72 h with either mock (−) or 1.0 μM DAC. The integrity of the cDNA was assessed by comparing the CT values for the genes of interest with that of GAPDH. *Columns* means of three experiments, *bars* SE

We next performed bisulfite-sequencing analysis to obtain detailed methylation profiles of the CpG sites in the region around the transcription start site of DFNA5 gene. We examined 45 CpG sites and found that DFNA5 was densely methylated in MCF7 cells, which do not express DFNA5. By contrast, little or no methylation was detected in MDA-MB435s, MDA-MB436, MDA-MB-468, and SK-Br-3 cells, which do express DFNA5 (Fig. 3). Thus, the results obtained with bisulfite-sequencing are consistent with both the bisulfite-pyrosequencing data and the DFNA5 expression status.

## Restoration of p53-dependent transcription of DFNA5 by demethylation

It was recently reported that DFNA5 is a target gene for p53 [36]. We therefore tested whether demethylation of DFNA5 in MCF7 cells would restore its transcriptional activation by p53 and/or by two other p53 family genes, TAp63$\gamma$ and TAp73$\beta$. When cells were infected with Ad-p53, Ad-p63$\gamma$, or Ad-p73$\beta$, expression of FLAG-tagged p53 family proteins was detected (Fig. 4a). In addition, p21, a cyclin-dependent inhibitor, was induced by all three vectors (Fig. 4a). We then examined expression of DFNA5 in MCF7 cells with or without treatment with DAC. We found that treating MCF7 cells with DAC restored induction of DFNA5 by p53 family genes, especially by p63, suggesting that DFNA5 is a target of the p53 family, not specifically p53, itself (Fig. 4b). We then performed ChIP assays to determine whether p63$\gamma$ directly interacts with the p53 response element of DFNA5 (RE-DFNA5) (Fig. 4c). PCR amplification of the ChIP products revealed that one DNA fragment containing RE-DFNA5 was present in the immunoprecipitated complex with p63$\gamma$. As a control, we confirmed that p63$\gamma$ binds to the p53 response element of MDM2 in vivo. These results indicate that DFNA5 can be upregulated by p63$\gamma$ through direct interaction with RE-DFNA5.

## Tumor suppressive activity of NTN4

Netrins and their receptors have been shown to be involved in tumorigenesis [37]. To test whether NTN4 suppresses growth of breast cancer cells, we performed colony formation assays using MCF7 cells, which express negligible levels NTN4. We found that introduction of a plasmid

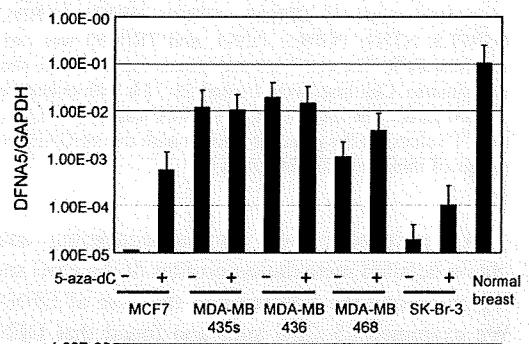
DFNA5/GAPDH
1.00E-00
1.00E-01
1.00E-02
1.00E-03
1.00E-04
1.00E-05
5-aza-dC
MCF7
MDA-MB 435s
MDA-MB 436
MDA-MB 468
SK-Br-3
Normal breast

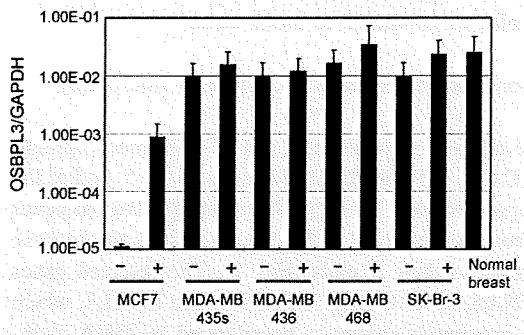
OSBPL3/GAPDH
1.00E-01
1.00E-02
1.00E-03
1.00E-04
1.00E-05
MCF7
MDA-MB 435s
MDA-MB 436
MDA-MB 468
SK-Br-3
Normal breast

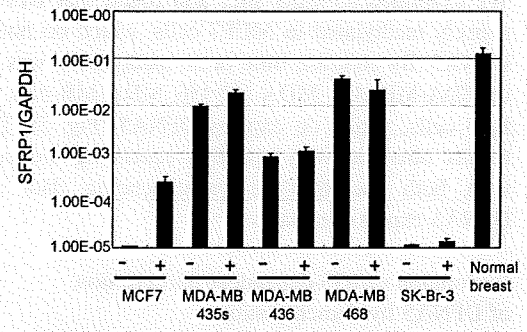
SFRP1/GAPDH
1.00E-00
1.00E-01
1.00E-02
1.00E-03
1.00E-04
1.00E-05
MCF7
MDA-MB 435s
MDA-MB 436
MDA-MB 468
SK-Br-3
Normal breast

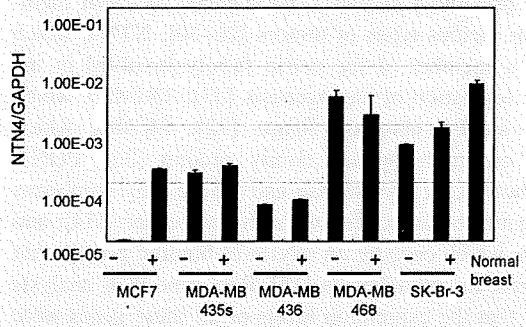
NTN4/GAPDH
1.00E-01
1.00E-02
1.00E-03
1.00E-04
1.00E-05
MCF7
MDA-MB 435s
MDA-MB 436
MDA-MB 468
SK-Br-3
Normal breast

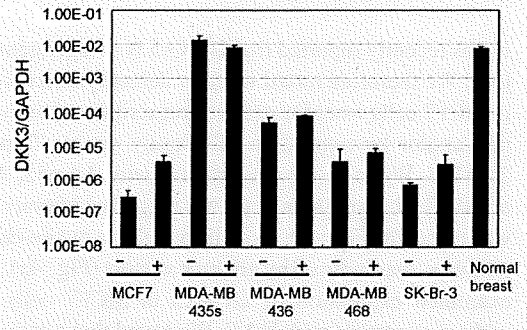
DKK3/GAPDH
1.00E-01
1.00E-02
1.00E-03
1.00E-04
1.00E-05
1.00E-06
1.00E-07
1.00E-08
MCF7
MDA-MB 435s
MDA-MB 436
MDA-MB 468
SK-Br-3
Normal breast

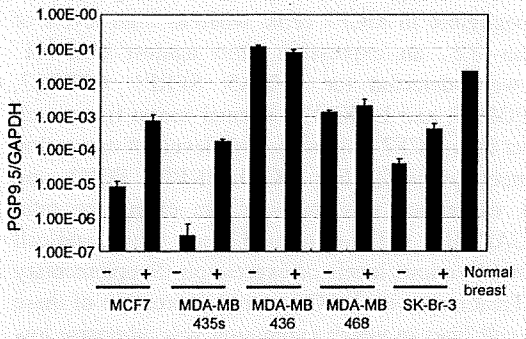
PGP9.5/GAPDH
1.00E-00
1.00E-01
1.00E-02
1.00E-03
1.00E-04
1.00E-05
1.00E-06
1.00E-07
MCF7
MDA-MB 435s
MDA-MB 436
MDA-MB 468
SK-Br-3
Normal breast

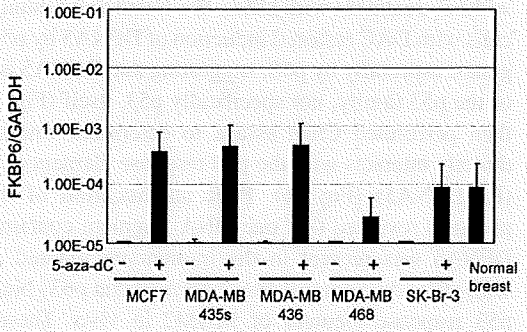
FKBP6/GAPDH
1.00E-01
1.00E-02
1.00E-03
1.00E-04
1.00E-05
5-aza-dC
MCF7
MDA-MB 435s
MDA-MB 436
MDA-MB 468
SK-Br-3
Normal breast

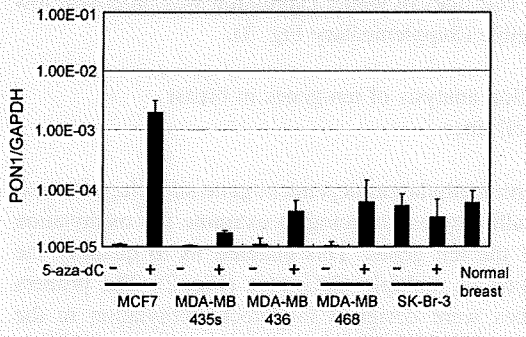
PON1/GAPDH
1.00E-01
1.00E-02
1.00E-03
1.00E-04
1.00E-05
5-aza-dC
MCF7
MDA-MB 435s
MDA-MB 436
MDA-MB 468
SK-Br-3
Normal breast

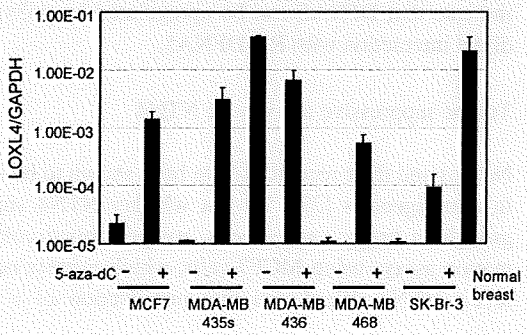
LOXL4/GAPDH
1.00E-01
1.00E-02
1.00E-03
1.00E-04
1.00E-05
5-aza-dC
MCF7
MDA-MB 435s
MDA-MB 436
MDA-MB 468
SK-Br-3
Normal breast

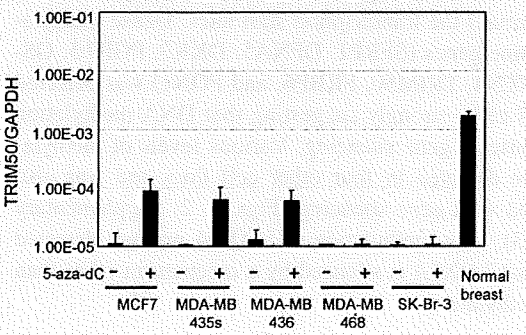
TRIM50/GAPDH
1.00E-01
1.00E-02
1.00E-03
1.00E-04
1.00E-05
5-aza-dC
MCF7
MDA-MB 435s
MDA-MB 436
MDA-MB 468
SK-Br-3
Normal breast

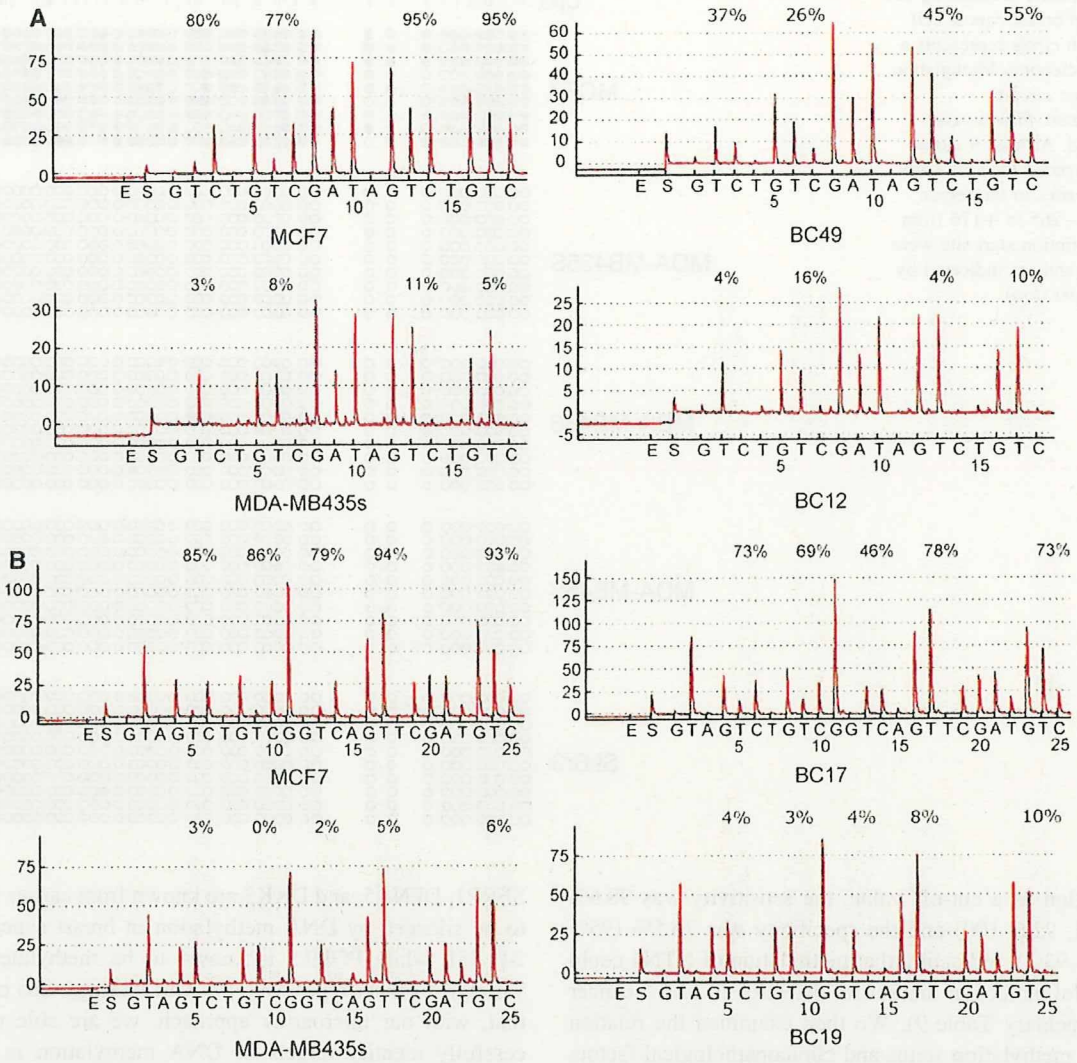


**Fig. 2** Representative results of bisulfite-pyrosequencing of DFNA5 (**a**) and SFRP1 (**b**). Bisulfite-pyrosequencing was carried out using DNA from breast cancer cell lines and primary breast cancer specimens. Examined were the regions upstream from the transcription start site (DFNA5: −85 to −97; SFRP1: −65 bp to −44 bp). *Gray columns* depict regions of CpG sites, and the percentage methylation at each CpG site is shown on the *top*. *Y*-axis, signal peaks expressed as a proportion of the number of nucleotides incorporated. *X*-axis, the nucleotides incorporated. Cell lines and specimens are shown below the *columns*

containing NTN4 cDNA significantly suppressed colony growth, suggesting that NTN4 does indeed have tumor suppressive activity (Fig. 5a, b).

## Comparison of methylation and clinicopathological features of patients with primary breast cancer

Of the nine aforementioned genes silenced by DNA methylation in primary breast cancer, seven showed significantly higher levels of methylation in cancerous tissues than in normal breast tissues ($P < 0.001$ for NTN4, PGP9.5, DKK3, OSBPL3, SFRP1, DFNA5; $P < 0.01$ for PON1, Fig. 6a; Supplementary Table 7). Methylation was also examined in paired samples of cancerous and adjacent normal breast tissues from 15 patients. Methylation of NTN4 ($P < 0.001$), PGP9.5 ($P < 0.001$), DKK3 ($P = 0.006$), and PON1 ($P = 0.031$) was significantly higher in the tumor tissue than in the adjacent breast tissue (Fig. 6b; Supplementary Table 8). The clinical usefulness of DNA methylation in distinguishing breast cancer from noncancerous tissue was confirmed by analyzing ROC curves (Fig. 6c; Supplementary Table 9). Methylation of NTN4, DKK3, and PGP9.5 showed highly discriminative ROC curve profiles, which clearly distinguished breast cancer from normal breast tissue (NTN4: $p < 0.001$; DKK3: $P < 0.001$; PGP9.5: $P < 0.001$). When we used 16%

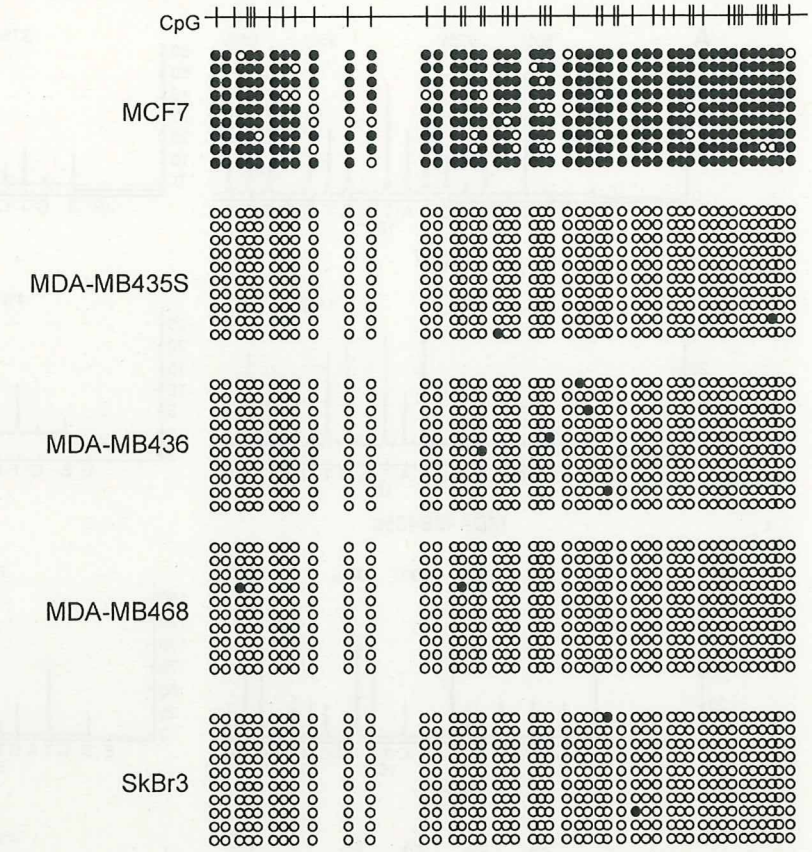


**Fig. 3** Bisulfite-sequencing of DFNA5 in breast cancer cell lines. Each *circle* represents a CpG dinucleotide. Methylation status: *open circles* unmethylated, *filled circles* methylated. At least 9 clones were sequenced for each case. The CpG sites in the region spanning −265 to +176 from the transcription start site were analyzed, and are indicated by vertical *bars* (*top*)

methylation as a cut-off value, the sensitivity was 98.6% (95% CI: 92.6–100) and the specificity was 76.5% (95% CI: 50.1–93.2), indicating that methylation of NTN4 could be a useful molecular marker for detection of breast cancer (Supplementary Table 9). We then examined the relation between methylation status and clinicopathological factors (Supplementary Table 10) and found that methylation of FKBP6 is significantly correlated with advanced stages (Fig. 7a; Supplementary Table 11, $P = 0.014$) and tumor size (Fig. 7b, Supplementary Table 12, $P = 0.017$). There was no correlation between methylation and other factors including stages, histological types, number of metastasis positive lymph nodes, vascular invasion.

## Discussion

### Identification of genes silenced by DNA methylation in breast cancer

In the present study, we performed a microarray analysis to identify genes silenced by DNA methylation in breast cancer. We found that 288 genes were upregulated more than fivefold after treatment with DAC. Among those, SFRP1, DFNA5, and DKK3 are known from earlier studies to be silenced by DNA methylation in breast cancer [23, 24, 38], while PGP9.5 is known to be methylated in a variety of cancer types [39, 40]. Our findings thus confirm that, with our microarray approach, we are able to successfully identify targets of DNA methylation in breast cancer. Gene ontology analysis revealed that genes involved in immune responses, the extracellular region and cytokine activity are significantly upregulated by DAC. Consistent to those findings, Karpf et al. [41] showed that genes regulated via interferon signaling are frequently upregulated by DAC, which suggests that upregulation of genes involved in immune responses, including those involved in antigen presentation, regulation of tumor necrosis factor and/or interferon pathways, may be a general feature of DAC treatment.

### Utility of DNA methylation for molecular diagnosis in breast cancer

Although previous studies have identified numerous targets of DNA methylation in breast cancer, the usefulness of the targeted genes for diagnosis remains unclear [13–15]. In fact, those studies confirmed DNA methylation of only a

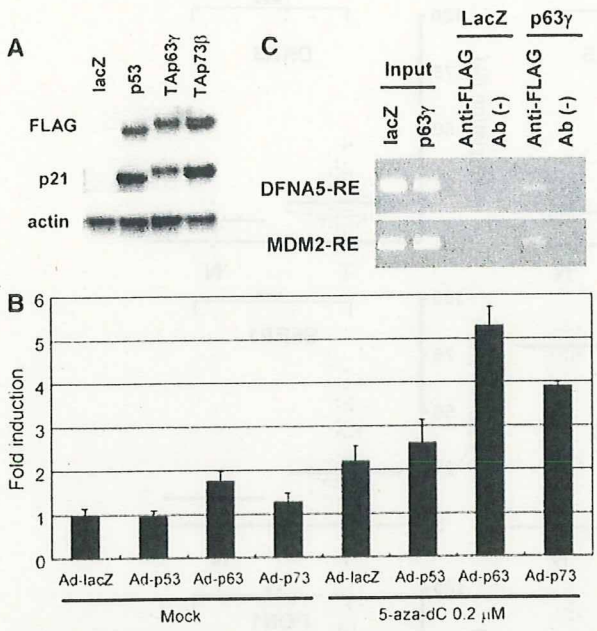


**Fig. 4** Induction of DFNA5 by p53 family members. **a** Western blot analysis of p53, TAp63$\gamma$, and TAp73$\beta$. MCF7 cells were infected with adenoviral vector encoding the protein shown on the *top* and were harvested 24 h after infection. Immunoblot analysis was performed using anti-FLAG antibody. Expression of p21 was examined as a control. **b** ChIP assay. PCR was performed using ChIP products, and one DNA fragment containing the RE-DFNA5 was present in the immunoprecipitated complex with TAp63$\gamma$. As a control, fragments MDM2 DNA were amplified. **c** Restoration of p53-dependent DFNA5 expression by DAC. MCF7 cells were treated for 72 h with either mock or 0.2 μM DAC followed by infection with 100 MOI of Ad-lacZ, Ad-p53, Ad-63$\gamma$, or Ad-p73$\beta$ for 24 h. Expression of DFNA5 was examined by real-time PCR. *Columns* mean of three experiments, *bars* SE

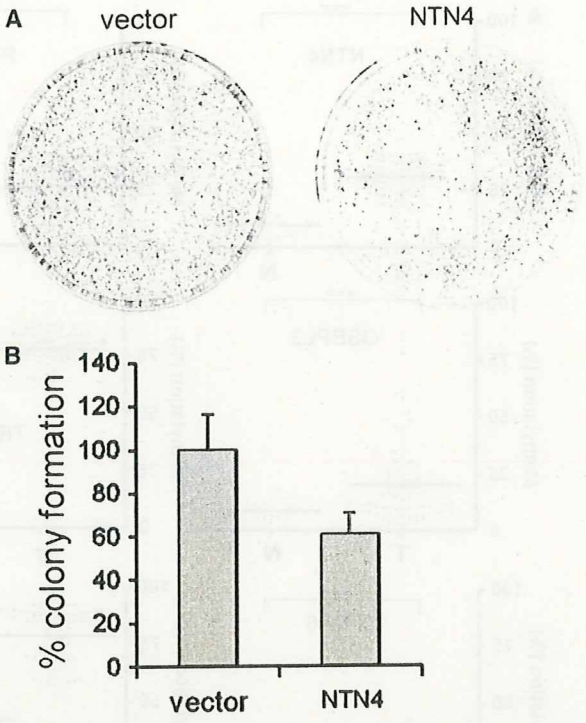


**Fig. 5** NTN4 suppresses breast cancer cell growth. **a** Colony formation assay. MCF7 cells were transfected with NTN4 or control vector and plated. After 2 weeks, the cells were fixed with methanol and stained with Giemsa. **b** Relative colony formation efficiencies of MCF7 cells transfected with NTN4 or control plasmid (vector). *Columns* mean of three experiments, *bars* SE

limited number of samples [13, 15], or the methylation analysis was not quantitative [14]. Our findings suggest DNA methylation can be used as a biomarker to detect breast cancer. The cancer can be detected using DNA from biopsy specimens, serum or breast fluid—i.e., any tissue in which genes specifically methylated at a high frequency in cancer can be identified. In the present study, bisulfite-pyrosequencing, a semi-quantitative methylation analysis, revealed that methylation of NTN4, PGP9.5, and DKK3 occurs in a cancer-specific manner. Previous studies have shown that PGP9.5 is silenced by DNA methylation in a variety of tumors [27, 39, 40], and cancer-specific methylation of PGP9.5 has been observed in both head/neck and hepatocellular cancers [39]. On the other hand, normal tissues in the prostate, esophagus, and stomach also show PGP9.5 methylation [39], so that whether or not methylation is cancer-specific is dependent on the cancer and tissue type. Recently, Veeck et al. [24] used methylation-specific PCR to assess the methylation of DKK3 and found that the gene is methylated in 61% of breast cancers. In the present study, we similarly observed that methylation of DKK3 is significantly higher in breast cancers (17.2%) than in normal breast tissues (17.2 vs. 9.8%, $P < 0.001$). Moreover, we showed for the first time that NTN4 is silenced by DNA methylation in cancer. When we used 16% methylation as a cut-off value, the sensitivity was 98.6% (95% CI: 92.6–100) and specificity was 76.5% (95% CI: 50.1–93.2), indicating that methylation of NTN4 could be a good molecular marker for detection of breast cancer.

In contrast to the genes mentioned above, methylation of FKBP6, PON1, and TRIM50 was detected even in normal breast tissues, and increases in promoter methylation reportedly correlate with age in colorectal and prostate tissues [42, 43]. In this regard, methylation of SFRP1, which has been shown to correlate with aging in colon [44], was not high in breast tissue, indicating that age-related methylation is also tissue-specific and that further studies

**Fig. 6** Methylation analysis in primary breast cancers. **a** Summary of methylation levels in normal and cancerous breast tissue: *N* normal tissue, *T* cancerous tissue. *** $P < 0.001$, ** $P < 0.01$. **b** Analysis of NTN4, PGP9.5, DKK3, and PON1 methylation in breast cancer and adjacent normal breast tissue. **c** ROC curve analysis of NTN4, PGP9.5, and DKK3 in primary breast cancer. The area under the ROC curve for each site conveys its utility for distinguishing normal breast from breast cancer in terms of its sensitivity and specificity

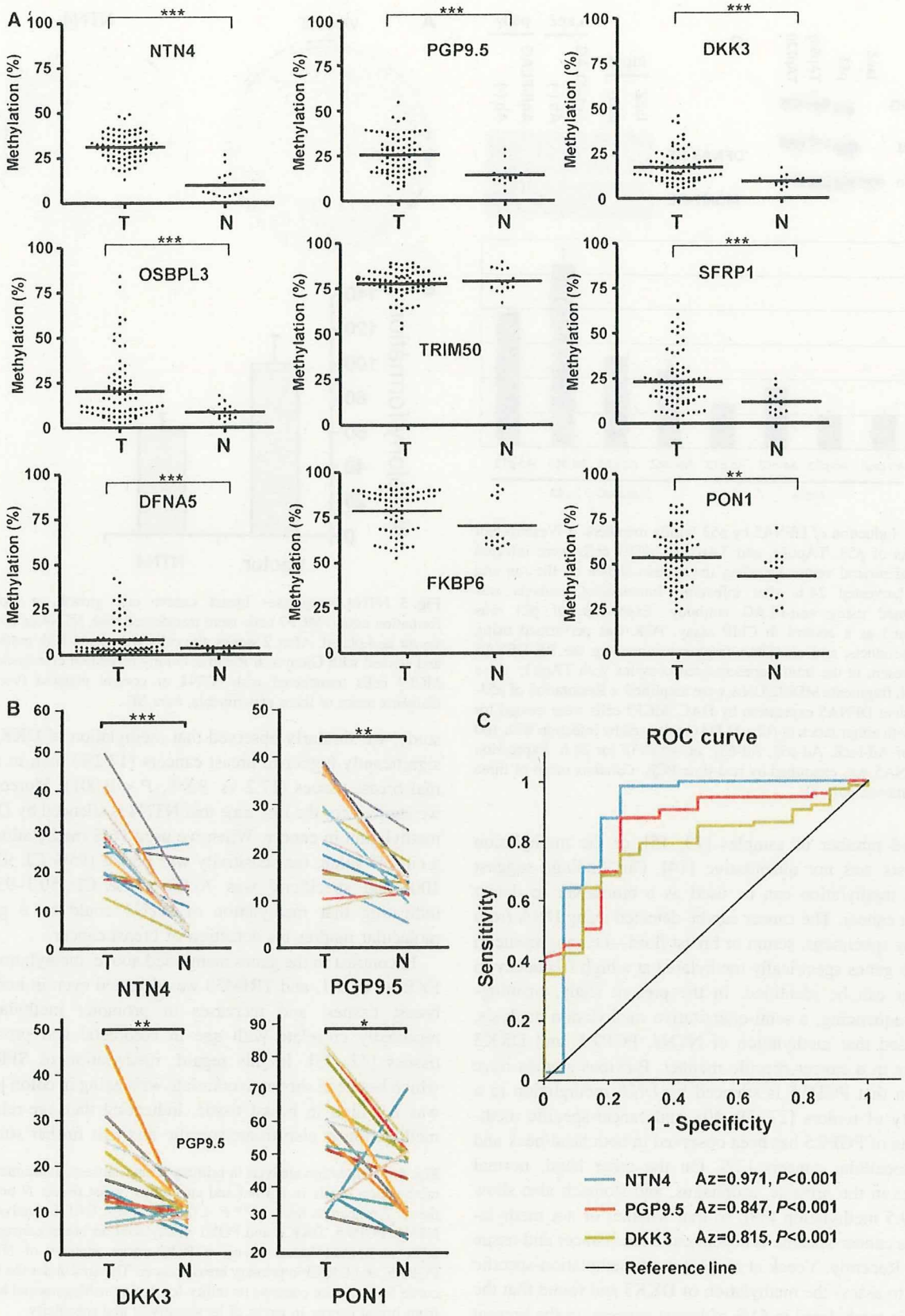
A
NTN4
PGP9.5
DKK3
OSBPL3
TRIM50
SFRP1
DFNA5
FKBP6
PON1
Methylation (%)
T
N
B
NTN4
PGP9.5
DKK3
PON1
C
ROC curve
Sensitivity
1 - Specificity
NTN4 Az=0.971, P<0.001
PGP9.5 Az=0.847, P<0.001
DKK3 Az=0.815, P<0.001
Reference line

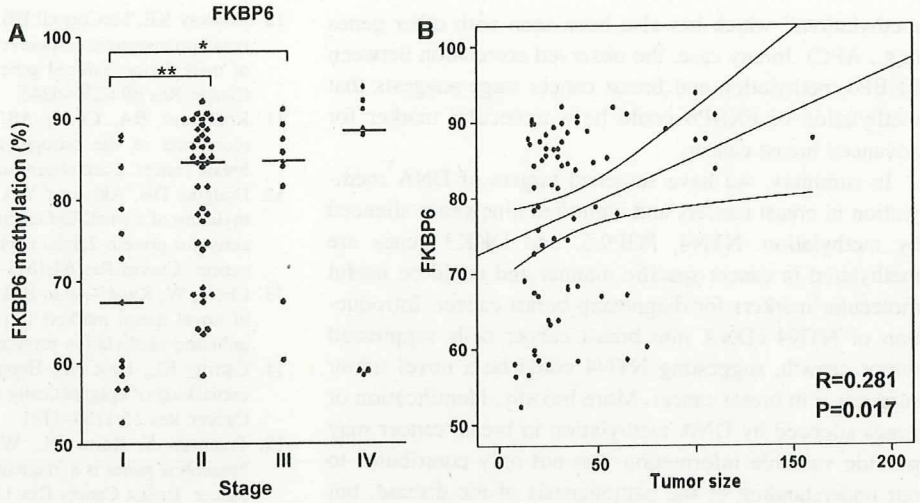


**Fig. 7** Correlation between FKBP6 methylation and the clinicopathological features of breast cancer. **a** Scatter plot of FKBP6 methylation in patients with cancers of different stages. ** $P < 0.01$, * $P < 0.05$. **b** Scatter plot in which FKBP6 methylation is plotted against tumor size. *X*-axis: tumor size (mm). *Y*-axis: FKBP6 methylation level (%)

will be necessary to clarify the significance of its methylation in normal breast tissues.

## Functional roles of genes silenced by DNA methylation in breast cancer

Our microarray analysis revealed several genes involved in cell signaling pathways to be methylated. SFRP1 and DKK3 are Wnt antagonists frequently silenced by methylation in colorectal and gastric cancers [29, 45, 46], and several lines of evidence suggest that activation of Wnt signaling plays a key role in breast cancer. For example, Bafico et al. [47] found that the unphosphorylated form of $\beta$-catenin is frequently present in breast cancer cell lines, and that the Wnt ligands WNT-2, WNT-3, and WNT6 are frequently overexpressed in the same cell lines. Mutation of APC or $\beta$-catenin is rare in breast cancer, however, so that the mechanism underlying the activation of Wnt signaling in this disease is not fully understood [48]. In the present study, we found that SFRP1 is inactivated by DNA methylation in MCF7 cells, and that SFRP1 is methylated in 45 of the 75 (60%) primary breast cancers tested. Perhaps inactivation of negative regulators of Wnt is involved in activating Wnt signaling in breast cancer.

DFNA5 was originally identified as a gene involved in nonsyndromic hearing impairment [49]. Since then, DFNA5 has also been identified as a gene downregulated in etoposide-resistant melanoma [50]. Although the role of DFNA5 in mediating the effects of etoposide remains unclear, Lage et al. [51] showed that introduction of the gene into tumor cells increases their susceptibility to apoptosis mediated by activated caspase-3 following etoposide treatment. In addition, DFNA5 was recently found to be inactivated by DNA methylation in gastric cancers, and introduction of DFNA5 into gastric cancer cells suppressed colony formation and induced apoptosis [26].

DFNA5 is reportedly a target gene of p53 [36]. In the present study, we found that DFNA5 is silenced by methylation in MCF7 cells and that treating the cells with DAC restored induction of DFNA5 by p53 family genes, especially p63$\gamma$. Thus, DFNA5 does not appear to be targeted selectively by p53, itself, but by p53 family member, p63$\gamma$.

Netrins are secreted molecules involved in axon guidance and angiogenesis. Among them, NTN4 is an antiangiogenic factor that acts through its receptor, neogenin [31]. Notably, expression of NTN4 is associated with a good prognosis in breast cancer [52]. In the present study, we showed for the first time that NTN4 is silenced by DNA methylation in breast cancer and that treating breast cancer cells with a demethylating agent (DAC) restores its expression. We also showed that NTN4 has tumor suppressive activity. Identification of NTN4 as a candidate tumor suppressor in breast cancer may be useful for the development of new cancer therapies [53]. The methylation of NTN4 was cancer-specific, suggesting epigenetic changes to the gene could be a useful molecular marker for diagnosis.

FK506-binding proteins (FKBPs) are immunophilins involved in protein folding and cell signaling. Among them, FKBP6 has been identified as a candidate gene underlying Williams syndrome, a developmental disorder caused by haploinsufficiency of genes at 7q11.23 [54], and expression of FKBP6 specifically localizes to meiotic chromosome cores and regions of homologous chromosome synapsis [33]. We found that methylation of FKBP6 was correlated with tumor size and stage. The role of FKBP6 in tumorigenesis remains unknown, but its methylation in normal tissue suggests that methylation of FKBP6 could be an example of so called "passenger

methylation," which has also been seen with other genes (e.g., APC). In any case, the observed correlation between FKBP6 methylation and breast cancer stage suggests that methylation of FKBP6 could be a molecular marker for advanced breast cancer.

In summary, we have screened targets of DNA methylation in breast cancers and identified nine genes silenced by methylation. NTN4, PGP9.5, and DKK3 genes are methylated in cancer-specific manner and could be useful molecular markers for diagnosing breast cancer. Introduction of NTN4 cDNA into breast cancer cells suppressed tumor growth, suggesting NTN4 could be a novel tumor suppressor in breast cancer. More broadly, identification of genes silenced by DNA methylation in breast cancer may provide valuable information that not only contributes to our understanding of the pathogenesis of the disease, but also to the development of new strategies for diagnosis and therapy.

**Acknowledgments** The authors thank Dr. William F. Goldman for editing the manuscript. This study was supported in part by Grants-in-Aid for Scientific Research on Priority Areas from the Ministry of Education, Culture, Sports, Science, and Technology (K.I., T.T., and M.T.), Grants-in-Aid for Scientific Research (S) from Japan Society for Promotion of Science (K.I.), a Grant-in-Aid for the Third-term Comprehensive 10-year Strategy for Cancer Control, and Grant-in-Aid for Cancer Research from the Ministry of Health, Labor, and Welfare, Japan (M.T.).

## References

1. Bird A (1992) The essentials of DNA methylation. Cell 70:5–8
2. Jones PA, Baylin SB (2007) The epigenomics of cancer. Cell 128:683–692
3. Jemal A, Siegel R, Ward E et al (2008) Cancer statistics, 2008. CA Cancer J Clin 58:71–96
4. Schuebel KE, Chen W, Cope L et al (2007) Comparing the DNA hypermethylome with gene mutations in human colorectal cancer. PLoS Genet 3:1709–1723
5. Herman JG, Merlo A, Mao L et al (1995) Inactivation of the CDKN2/p16/MTS1 gene is frequently associated with aberrant DNA methylation in all common human cancers. Cancer Res 55:4525–4530
6. Ferguson AT, Evron E, Umbricht CB et al (2000) High frequency of hypermethylation at the 14-3-3 sigma locus leads to gene silencing in breast cancer. Proc Natl Acad Sci USA 97:6049–6054
7. Graff JR, Herman JG, Lapidus RG et al (1995) E-cadherin expression is silenced by DNA hypermethylation in human breast and prostate carcinomas. Cancer Res 55:5195–5199
8. Krop IE, Sgroi D, Porter DA et al (2001) HIN-1, a putative cytokine highly expressed in normal but not cancerous mammary epithelial cells. Proc Natl Acad Sci USA 98:9796–9801
9. Dammann R, Yang G, Pfeifer GP (2001) Hypermethylation of the cpG island of Ras association domain family 1A (RASSF1A), a putative tumor suppressor gene from the 3p21.3 locus, occurs in a large percentage of human breast cancers. Cancer Res 61:3105–3109
10. Conway KE, McConnell BB, Bowring CE et al (2000) TMS1, a novel proapoptotic caspase recruitment domain protein, is a target of methylation-induced gene silencing in human breast cancers. Cancer Res 60:6236–6242
11. Rodriguez BA, Cheng AS, Yan PS et al (2008) Epigenetic repression of the estrogen-regulated Homeobox B13 gene in breast cancer. Carcinogenesis 29:1459–1465
12. Douglas DB, Akiyama Y, Carraway H et al (2004) Hypermethylation of a small CpGuanine-rich region correlates with loss of activator protein-2alpha expression during progression of breast cancer. Cancer Res 64:1611–1620
13. Chung W, Kwabi-Addo B, Ittmann M et al (2008) Identification of novel tumor markers in prostate, colon and breast cancer by unbiased methylation profiling. PLoS One 3:e2079
14. Ostrow KL, Park HL, Hoque MO et al (2009) Pharmacologic unmasking of epigenetically silenced genes in breast cancer. Clin Cancer Res 15:1184–1191
15. Tommasi S, Karm DL, Wu X et al (2009) Methylation of homeobox genes is a frequent and early epigenetic event in breast cancer. Breast Cancer Res 11:R14
16. Gardiner-Garden M, Frommer M (1987) CpG islands in vertebrate genomes. J Mol Biol 196:261–282
17. Clark SJ, Harrison J, Paul CL et al (1994) High sensitivity mapping of methylated cytosines. Nucleic Acids Res 22:2990–2997
18. Watanabe Y, Toyota M, Kondo Y et al (2007) PRDM5 identified as a target of epigenetic silencing in colorectal and gastric cancer. Clin Cancer Res 13:4786–4794
19. Yang AS, Estecio MR, Doshi K et al (2004) A simple method for estimating global DNA methylation using bisulfite PCR of repetitive DNA elements. Nucleic Acids Res 32:e38
20. Sasaki Y, Morimoto I, Ishida S et al (2001) Adenovirus-mediated transfer of the p53 family genes, p73 and p51/p63 induces cell cycle arrest and apoptosis in colorectal cancer cell lines: potential application to gene therapy of colorectal cancer. Gene Ther 8:1401–1408
21. Sasaki Y, Negishi H, Koyama R et al (2009) p53 family members regulate the expression of the apolipoprotein D gene. J Biol Chem 284:872–883
22. Suzuki H, Igarashi S, Nojima M et al (2009) IGFBP7 is a p53 responsive gene specifically silenced in colorectal cancer with CpG island methylator phenotype. Carcinogenesis. doi:10.1093/carcin/bgp179
23. Kim MS, Lebron C, Nagpal JK et al (2008) Methylation of the DFNA5 increases risk of lymph node metastasis in human breast cancer. Biochem Biophys Res Commun 370:38–43
24. Veeck J, Bektas N, Hartmann A et al (2008) Wnt signalling in human breast cancer: expression of the putative Wnt inhibitor Dickkopf-3 (DKK3) is frequently suppressed by promoter hypermethylation in mammary tumours. Breast Cancer Res 10:R82
25. Veeck J, Niederacher D, An H et al (2006) Aberrant methylation of the Wnt antagonist SFRP1 in breast cancer is associated with unfavourable prognosis. Oncogene 25:3479–3488
26. Akino K, Toyota M, Suzuki H et al (2007) Identification of DFNA5 as a target of epigenetic inactivation in gastric cancer. Cancer Sci 98:88–95
27. Mandelker DL, Yamashita K, Tokumaru Y et al (2005) PGP9.5 promoter methylation is an independent prognostic factor for esophageal squamous cell carcinoma. Cancer Res 65:4963–4968
28. Sato H, Suzuki H, Toyota M et al (2007) Frequent epigenetic inactivation of DICKKOPF family genes in human gastrointestinal tumors. Carcinogenesis 28:2459–2466
29. Suzuki H, Watkins DN, Jair KW et al (2004) Epigenetic inactivation of SFRP genes allows constitutive WNT signaling in colorectal cancer. Nat Genet 36:417–422

30. Wu G, Guo Z, Chang X et al (2007) LOXL1 and LOXL4 are epigenetically silenced and can inhibit ras/extracellular signal-regulated kinase signaling pathway in human bladder cancer. Cancer Res 67:4123–4129
31. Lejmi E, Leconte L, Pedron-Mazoyer S et al (2008) Netrin-4 inhibits angiogenesis via binding to neogenin and recruitment of Unc5B. Proc Natl Acad Sci USA 105:12491–12496
32. Micale L, Fusco C, Augello B et al (2008) Williams-Beuren syndrome TRIM50 encodes an E3 ubiquitin ligase. Eur J Hum Genet 16:1038–1049
33. Crackower MA, Kolas NK, Noguchi J et al (2003) Essential role of Fkbp6 in male fertility and homologous chromosome pairing in meiosis. Science 300:1291–1295
34. Marchesani M, Hakkarainen A, Tuomainen TP et al (2003) New paraoxonase 1 polymorphism I102V and the risk of prostate cancer in Finnish men. J Natl Cancer Inst 95:812–818
35. Lehto M, Mayranpaa MI, Pellinen T et al (2008) The R-Ras interaction partner ORP3 regulates cell adhesion. J Cell Sci 121:695–705
36. Masuda Y, Futamura M, Kamino H et al (2006) The potential role of DFNA5, a hearing impairment gene, in p53-mediated cellular response to DNA damage. J Hum Genet 51:652–664
37. Arakawa H (2004) Netrin-1 and its receptors in tumorigenesis. Nat Rev Cancer 4:978–987
38. Suzuki H, Toyota M, Carraway H et al (2008) Frequent epigenetic inactivation of Wnt antagonist genes in breast cancer. Br J Cancer 98:1147–1156
39. Tokumaru Y, Yamashita K, Kim MS et al (2008) The role of PGP9.5 as a tumor suppressor gene in human cancer. Int J Cancer 123:753–759
40. Yamashita K, Park HL, Kim MS et al (2006) PGP9.5 methylation in diffuse-type gastric cancer. Cancer Res 66:3921–3927
41. Karpf AR, Peterson PW, Rawlins JT et al (1999) Inhibition of DNA methyltransferase stimulates the expression of signal transducer and activator of transcription 1, 2, and 3 genes in colon tumor cells. Proc Natl Acad Sci USA 96:14007–14012
42. Issa JP, Ahuja N, Toyota M et al (2001) Accelerated age-related CpG island methylation in ulcerative colitis. Cancer Res 61: 3573–3577
43. Kwabi-Addo B, Chung W, Shen L et al (2007) Age-related DNA methylation changes in normal human prostate tissues. Clin Cancer Res 13:3796–3802
44. Shen L, Toyota M, Kondo Y et al (2007) Integrated genetic and epigenetic analysis identifies three different subclasses of colon cancer. Proc Natl Acad Sci USA 104:18654–18659
45. Nojima M, Suzuki H, Toyota M et al (2007) Frequent epigenetic inactivation of SFRP genes and constitutive activation of Wnt signaling in gastric cancer. Oncogene 26:4699–4713
46. Rattner A, Hsieh JC, Smallwood PM et al (1997) A family of secreted proteins contains homology to the cysteine-rich ligand-binding domain of frizzled receptors. Proc Natl Acad Sci USA 94:2859–2863
47. Bafico A, Liu G, Goldin L et al (2004) An autocrine mechanism for constitutive Wnt pathway activation in human cancer cells. Cancer Cell 6:497–506
48. Schlosshauer PW, Brown SA, Eisinger K et al (2000) APC truncation and increased beta-catenin levels in a human breast cancer cell line. Carcinogenesis 21:1453–1456
49. Van Laer L, Huizing EH, Verstreken M et al (1998) Nonsyndromic hearing impairment is associated with a mutation in DFNA5. Nat Genet 20:194–197
50. Thompson DA, Weigel RJ (1998) Characterization of a gene that is inversely correlated with estrogen receptor expression (ICERE-1) in breast carcinomas. Eur J Biochem 252:169–177
51. Lage H, Helmbach H, Grottke C et al (2001) DFNA5 (ICERE-1) contributes to acquired etoposide resistance in melanoma cells. FEBS Lett 494:54–59
52. Esseghir S, Kennedy A, Seedhar P et al (2007) Identification of NTN4, TRA1, and STC2 as prognostic markers in breast cancer in a screen for signal sequence encoding proteins. Clin Cancer Res 13:3164–3173
53. Toyota M, Suzuki H, Yamashita T et al (2009) Cancer epigenomics: implications of DNA methylation in personalized cancer therapy. Cancer Sci 100:787–791
54. Meng X, Lu X, Morris CA et al (1998) A novel human gene FKBP6 is deleted in Williams syndrome. Genomics 52:130–137

Carcinogenesis vol.31 no.3 pp.342–349, 2010
doi:10.1093/carcin/bgp179
*Advance Access publication July 28, 2009*

# IGFBP7 is a p53-responsive gene specifically silenced in colorectal cancer with CpG island methylator phenotype

**Hiromu Suzuki[1,2,3], Shinichi Igarashi[1], Masanori Nojima[4], Reo Maruyama[1], Eiichiro Yamamoto[1], Masahiro Kai[2], Hirofumi Akashi[5], Yoshiyuki Watanabe[6], Hiroyuki Yamamoto[1], Yasushi Sasaki[3], Fumio Itoh[6], Kohzoh Imai[1], Tamotsu Sugai[7], Lanlan Shen[8], Jean-Pierre J.Issa[8], Yasuhisa Shinomura[1], Takashi Tokino[3] and Minoru Toyota[2,*]**

[1]First Department of Internal Medicine, [2]Department of Biochemistry, [3]Department of Molecular Biology, Cancer Research Institute, [4]Department of Public Health and [5]Center for Bioinformation, Sapporo Medical University, South 1,West 17, Chuo-ku, Sapporo 060-8556, Japan, [6]Department of Gastroenterology and Hepatology, St Marianna University School of Medicine, Kawasaki 216-8511, Japan, [7]Division of Diagnostic Molecular Pathology, Department of Pathology, Iwate Medical University, Morioka 020-8505, Japan and [8]Department of Leukemia and Epigenetics Center, University of Texas M. D. Anderson Cancer Center, Houston, TX 77030, USA

*To whom correspondence should be addressed. Tel: +81 11 611 2111 ext. 2680; Fax: +81 11 622 1918;
Email: mtoyota@sapmed.ac.jp
Correspondence may also be addressed to Yasuhisa Shinomura.
Tel: +81 11 611 2111 ext. 3210; Fax: +81 11 611 2282;
Email: shinomura@sapmed.ac.jp

**A subset of colorectal cancers (CRCs) show simultaneous methylation of multiple genes; these tumors have the CpG island methylator phenotype (CIMP). CRCs with CIMP show a specific pattern of genetic alterations, including a high frequency of *BRAF* mutations and a low frequency of *p53* mutations. We therefore hypothesized that genes inactivated by DNA methylation are involved in the BRAF- and p53-signaling pathways. Among those, we examined the epigenetic inactivation of insulin-like growth factor-binding protein 7 (*IGFBP7*) expression in CRCs. We found that in CRC cell lines, the silencing of *IGFBP7* expression was correlated with high levels of DNA methylation and low levels of histone H3K4 methylation. Luciferase and chromatin immunoprecipitation assays in unmethylated cells revealed that p53 induces expression of *IGFBP7* upon binding to a p53 response element within intron 1 of the gene. Treating methylated CRC cell lines with 5-aza-2′-deoxycytidine restored p53-induced *IGFBP7* expression. Levels of *IGFBP7* methylation were also significantly higher in primary CRC specimens than in normal colonic tissue ($P < 0.001$). Methylation of *IGFBP7* was correlated with BRAF mutations, an absence of p53 mutations and the presence of CIMP. Thus, epigenetic inactivation of *IGFBP7* appears to play a key role in tumorigenesis of CRCs with CIMP by enabling escape from p53-induced senescence.**

## Introduction

Colorectal cancer (CRC) arises through the accumulation of multiple genetic changes, including mutation of *APC*, *K-ras* and *p53* (1). In addition to genetic changes, however, epigenetic alterations such as DNA methylation also play a role through the silencing of cancer-related genes (2–4). Moreover, a subset of CRCs show methylation of multiple genes, which has been termed the CpG island methylator phenotype (CIMP, ref. 5). Tumors with CIMP show distinct pattern of genetic alterations, including a high frequency of *K-ras* and *BRAF* mutations and a low frequency of *p53* mutations (6–8). The molecular mechanism underlying this pattern of mutations remains unknown.

Senescence is a state of permanent growth arrest in which cells are refractory to mitogenic stimuli. Although activation of Ras exerts a mitogenic effect in immortalized cells, expression of oncogenic Ras provokes stress responses in primary cells that results in irreversible growth arrest termed premature senescence (9,10). In most cell types, activation of p53 is crucial for initiating senescence in response to DNA damage, and it has been shown that p53-mediated senescence is caused by induction of target genes such as *p21WAF1/CDKN1A*, *PAI-1* and *DEC-1* (11,12).

p53 is a transcription factor that induces expression of various genes involved in cell cycle checkpoints, apoptosis and DNA repair (13), and a variety of approaches, including differential display, representational difference analysis and complementary DNA (cDNA) microarray, have been used to identify its targets. p53 acts by binding to so-called p53 response elements (p53REs), which consist of two copies of a 10 bp motif, separated by 0–12 bp. Using the p53RE as a probe, we previously employed an in silico approach to identify the vitamin D receptor gene as a transcriptional target of p53 (14), which confirmed the utility of the in silico analysis for identification of p53 target genes within the human genome.

Insulin-like growth factor-binding protein 7 (IGFBP7; also called IGFBP-rl or MAC25) can inhibit proliferation of cancer cells, and its expression is downregulated in various types of tumors (15,16). For instance, *IGFBP7* is silenced by DNA methylation in both colorectal and gastric cancers (17,18). Although the function of IGFBP7 in tumorigenesis is not fully understood, Wajapeyee *et al.* (19) recently reported that expression of activated BRAF in primary melanocytes leads to synthesis of IGFBP7, which then acts through autocrine/paracrine pathways to inhibit extracellular signal-regulated kinase signaling and induce senescence and apoptosis in BRAF-activated cells. Our findings in the present study indicate that *IGFBP7* is a direct target of p53, suggesting that IGFBP7 is a mediator of p53-dependent growth suppression and that epigenetic inactivation of *IGFBP7* is a potentially useful molecular target for the diagnosis and treatment of CRCs with CIMP.

## Materials and methods

### *Cell lines and tissue specimens*

A set of nine CRC cell lines (CaCO2, Colo320, DLD1, HCT116, HT29, LoVo, RKO, SW48 and SW480) and a lung cancer cell line (H1299) were obtained and cultured as described previously (14,20). HCT116 cells harboring genetic disruptions within the *DNA methyltransferase 1 (DNMT1)* and *DNMT3B* loci (DKO2) (21) and within the *TP53* locus (22) have been described previously. A total of 87 primary CRCs, 49 colorectal adenoma and 41 normal colon specimens were collected as described previously (7). Informed consent was obtained from all patients before collection of the specimens. Genomic DNA was extracted using the standard phenol–chloroform procedure. Total RNA was extracted using TRIZOL reagent (Invitrogen, Carlsbad, CA) and then treated with a DNA-free kit (Ambion, Austin, TX). Genomic DNA and total RNA from normal colon tissue from a healthy individual were purchased from BioChain (Hayward, CA).

### *Drug treatment*

To analyze restoration of *IGFBP7* gene expression, CRC cells were treated with 2 μM 5-aza-2′-deoxycytidine (DAC) (Sigma, St Louis, MO) for 72 h, replacing the drug and medium every 24 h. To determine whether *IGFBP7* is upregulated by endogenous p53, wild-type and $p53^{-/-}$ HCT116 cells were treated with 0.1 μM DAC for 48 h, replacing the drug and medium 24 h after the beginning of treatment. This was followed by addition of adriamycin (ADR) to a final concentration of 0.5 μg/ml and incubation for an additional 24 h.

### *In silico identification of p53RE*

A p53RE database was created as described previously (14). Briefly, human genome sequence data were downloaded from the National Center for

**Abbreviations:** ADR, adriamycin; cDNA, complementary DNA; ChIP, chromatin immunoprecipitation; CIMP, CpG island methylator phenotype; CRC, colorectal cancer; DAC, 5-aza-2′-deoxycytidine; DNMT1, DNA methyltransferase 1; IGFBP7, insulin-like growth factor-binding protein 7; mRNA, messenger RNA; MSP, methylation-specific polymerase chain reaction; PCR, polymerase chain reaction; p53RE, p53 response element.

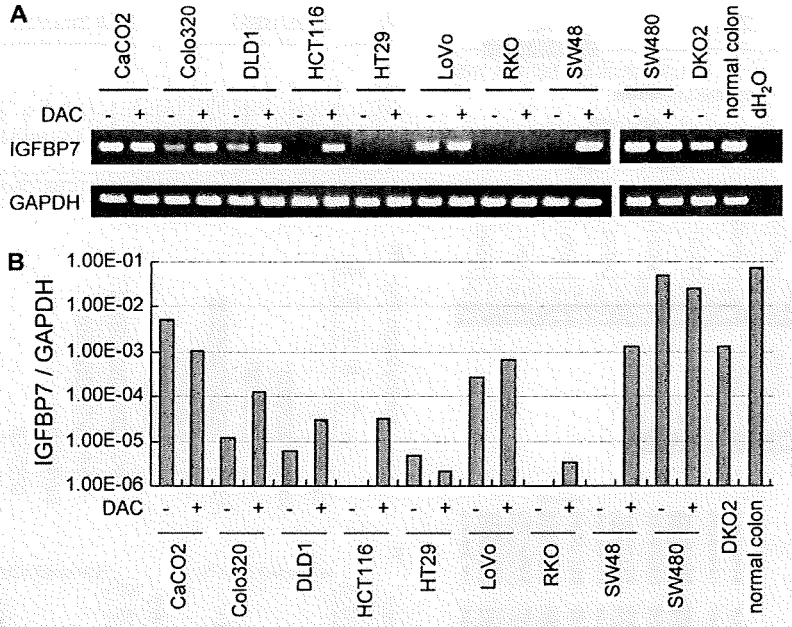


**Fig. 1.** Analysis of *IGFBP7* expression in CRC cell lines. (**A**) Reverse transcriptase–PCR analysis of *IGFBP7* in the indicated CRC cell lines. Expression of *IGFBP7* was examined using cDNA prepared from CRC cell lines treated with mock (−) or 1.0 μM DAC (+). Glyceraldehyde-3-phosphate dehydrogenase (GAPDH) expression was used as a control to confirm the integrity of the RNA. (**B**) Real-time PCR analysis of *IGFBP7*. The results were normalized using levels of glyceraldehyde-3-phosphate dehydrogenase expression as control.

Biotechnology Information Human Assembly 33. Stored in the p53RE database were sequences containing fewer than four mismatches in the 20 nucleotide p53RE consensus sequence and a spacer of fewer than 12 bp between the two 10 bp motifs. We then analyzed the distribution of p53REs with respect to transcription start sites for *IGFBP7*, taking into consideration the number of mismatches and the length of the spacers.

*Reverse transcriptase–polymerase chain reaction*

Single-stranded cDNA was prepared using SuperScript III reverse transcriptase (Invitrogen), and the integrity of the cDNA was confirmed by amplifying glyceraldehyde-3-phosphate dehydrogenase (*GAPDH*). Polymerase chain reaction (PCR) was run in a 50 μl volume containing 100 ng of cDNA, 1× Ex Taq Buffer (TaKaRa, Otsu, Japan), 0.3 mM deoxynucleoside triphosphate, 0.25 μM each primer and 1 U of TaKaRa Ex Taq Hot Start Version (TaKaRa). The PCR protocol entailed 5 min at 95°C; 35 cycles of 1 min at 95°C, 1 min at 55°C and 1 min at 72°C; and a 7 min final extension at 72°C. Primer sequences and PCR product sizes are shown in supplementary Table 1 (available at *Carcinogenesis* Online).

*Real-time reverse transcriptase–PCR*

Real-time reverse transcriptase–PCR was carried out using TaqMan Gene Expression Assays (Applied Biosystems, Carlsbad, CA) and 7900HT Fast Real-Time PCR System (Applied Biosystems) according to the manufacturer's instructions. SDS2.2.2 software (Applied Biosystems) was used for comparative ΔCt analysis, and *GAPDH* served as an endogenous control.

*Methylation analysis*

Genomic DNA (2 μg) was modified with sodium bisulfite using an EpiTect Bisulfite Kit (Qiagen, Hilden, Germany). Methylation-specific polymerase chain reaction (MSP) and bisulfite sequencing analysis were performed as described previously (23). Bisulfite sequencing and PCR products were cloned into pCR2.1-TOPO vector (Invitrogen), and 8–12 clones from each sample were sequenced using an ABI3130x automated sequencer (Applied Biosystems).

Bisulfite pyrosequencing was carried out as described previously (20) using primers designed with PSQ Assay Design software (Biotage, Uppsala, Sweden). After PCR, the biotinylated products were purified, made single stranded and used as a template in the pyrosequencing reaction run according to the manufacturer's instructions. The PCR products were bound to Streptavidin Sepharose beads HP (Amersham Biosciences, Piscataway, NJ), after which beads containing the immobilized PCR product were purified, washed and denatured using a 0.2 M NaOH solution. After addition of 0.3 μM sequencing primer to the purified PCR product, pyrosequencing was carried out using a PSQ96MA system (Biotage) and Pyro Q-CpG software (Biotage). Primer sequences and PCR product sizes are shown in supplementary Table 1 (available at *Carcinogenesis* Online).

*Chromatin immunoprecipitation*

Chromatin immunoprecipitation (ChIP) was carried out using a ChIP Assay Kit (Upstate Biotechnology, Lake Placid, NY) with anti-trimethylated histone H3K4 monoclonal antibody (clone MC315; Upstate, Lake Placid, NY) or anti-human p53 monoclonal antibody (DO-1; Santa Cruz Biotechnology, Santa Cruz, CA) as described previously (14,20,24). For histone methylation analysis, HCT116 cells treated with or without DAC and DKO2 cells were used as described previously (20). For p53 analysis, DLD1 cells infected with recombinant adenovirus Ad-p53 or Ad-LacZ were used (14). Briefly, the protein and DNA in $2 \times 10^6$ cells were cross-linked in a 1% formaldehyde solution for 15 min at 37°C. The cells were then lysed in 200 μl of sodium dodecyl sulfate lysis buffer and sonicated to generate 300–800 bp DNA fragments. After centrifugation, the cleared supernatant was diluted 10-fold with ChIP dilution buffer, after which one-fiftieth of the extract volume was used for PCR amplification as the input control. The remaining extract was incubated with specific antibody for 16 h at 4°C. Immune complexes were precipitated, washed and eluted as recommended. DNA–protein cross-links were reversed by heating for 4 h at 65°C, after which the DNA fragments were purified and dissolved in 50 μl of Tris–ethylenediaminetetraacetic acid. One microliter of each sample was used as a template for PCR amplification. Real-time PCR for histone analysis was carried as described previously (20) using the primers listed in supplementary Table 1 (available at *Carcinogenesis* Online). PCR amplification of *IGFBP7* containing the putative p53RE was also carried out using primers listed in supplementary Table 1 (available at *Carcinogenesis* Online).

*Luciferase assays*

Reporter plasmids pGL3-RE-*IGFBP7* and pGL3-RE-*IGFBP7*-mut were constructed as follows. Three tandem repeats of RE-*IGFBP7* (5′-AAACAAGTCCAAGCTTGCTG-3′) and its unresponsive mutant form, RE-*IGFBP7*-mut (5′-AAAAAATTCCAAGATTTCTG-3′), were synthesized and inserted upstream of a basal SV40 promoter in the pGL3-promoter vector (Promega, Madison, WI), yielding pGL3-RE-*IGFBP7* and pGL3-RE-*IGFBP7*-mut, respectively. Using Lipofectamine 2000 (Invitrogen), H1299 cells ($5 \times 10^4$ cells per well in 24-well plates) were transfected with 100 ng of one of the reporter plasmids, 100 ng of pcDNA-p53 or an empty vector and 2 ng of pRL-TK (Promega). Luciferase activities were measured 48 h after transfection using a Dual-Luciferase Reporter Assay System (Promega). The ability to stimulate transcription was determined

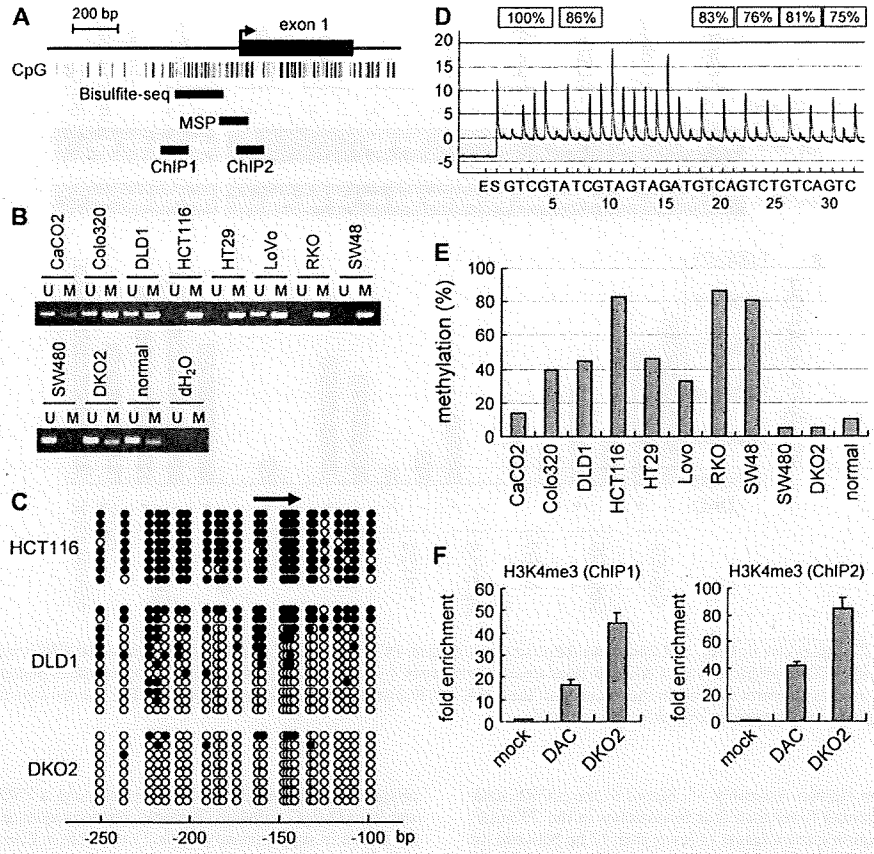


**Fig. 2.** Methylation analysis of *IGFBP7*. (**A**) Schematic representation of the 5′ region of *IGFBP7*. CpG sites are shown as vertical bars. The regions analyzed by bisulfite sequencing, MSP and ChIP are indicated by solid bars. The transcription start site is indicated by an arrow. (**B**) MSP analysis of *IGFBP7* in CRC cell lines. The cell lines examined are shown on the top. (**C**) Bisulfite sequencing of IGFBP7. Open and filled circles represent unmethylated and methylated CpG sites, respectively. (**D**) Representative pyrogram for *IGFBP7*. Gray columns indicate regions with C to T polymorphic sites. The percentage of methylation at each CpG site is shown at the top; *y*-axis, signal peaks proportional to the number of nucleotides incorporated and *x*-axis, the nucleotides incorporated. (**E**) Summary of pyrosequencing. *y*-axis, the percentages of methylated cytosines in the samples, as determined from pyrosequencing. (**F**) ChIP analysis of trimethylation of histone H3K4 in the 5′ region of IGFBP7. ChIP assays were performed using HCT116 cells treated with mock or DAC. DKO2 cells (*DNMT1*$^{-/-}$*DNMT3B*$^{-/-}$ HCT116 cells) were also used.

from the ratio of luciferase activity in the cells transfected with the pGL3-RE-*IGFBP7* to the activity in the cells transfected with pGL3-RE-*IGFBP7*-mut. All experiments were performed in triplicate and repeated at least three times.

*Expression vector*

Full-length *IGFBP7* cDNA was PCR amplified using cDNA derived from DKO2 cells as a template. The PCR was run in a 50 μl volume containing 1× AccuPrime *Pfx* Reaction mix (Invitrogen), 0.3 μM each primer and 2.5 U of AccuPrime *Pfx* DNA polymerase (Invitrogen). The PCR protocol entailed 2 min at 95°C; 35 cycles of 15 s at 95°C, 30 s at 62°C and 1 min at 68°C; and a 5 min final extension at 68°C. Primer sequences are listed in supplementary Table 1 (available at *Carcinogenesis* Online). Amplified PCR products were then incubated with 1 U of Ex Taq DNA Polymerase (TaKaRa) for 10 min and cloned into pCR2.1-TOPO (Invitrogen). After the sequences were verified, fragments were cut using EcoRI and ligated into EcoRI-digested pcDNA3.1/HisA (Invitrogen).

*Colony formation assays*

Colony formation assays were carried out as described previously (25). Briefly, cells ($1 \times 10^5$ cells) were transfected with 5 μg of one of the pcDNA3.1His-IGFBP7 vectors or with empty vector using Lipofectamine 2000 according to the manufacturer's instructions. Cells were then plated on 60 mm culture dishes and selected for 14 days with 0.6 mg/ml G418, after which the colonies that formed were stained with Giemsa and counted using National Institutes of Health IMAGE software.

*Statistics*

Statistical analyses were carried out using SPSSJ 15.0 (SPSS Japan, Tokyo, Japan). Pearson's correlation coefficient and *t*-test were used to evaluate the association between *IGFBP7* methylation. Methylation of *p16*, mutations of *p53*, mutations of *BRAF*, microsatellite instability and CIMP status were determined as described previously (5,7,26). Values of $P < 0.05$ were considered significant. To identify potentially distinct subgroups among colon cancer and adenoma patients, heat maps were constructed using K-means clustering method (27).

## Results

*Analysis of IGFBP7* expression in CRC cell lines

To test whether *IGFBP7* is epigenetically silenced in CRC, we first carried out an reverse transcriptase–PCR analysis with a set of CRC cell lines. We found that expression of *IGFBP7* messenger RNA (mRNA) was completely absent in four of the nine cell lines tested (HCT116, HT29, RKO and SW48) and was downregulated in two cell lines (Colo320 and DLD1) (Figure 1A). In many of the cells in which *IGFBP7* was downregulated, treatment with the DNA methyltransferase inhibitor DAC rapidly restored mRNA expression, which is indicative of epigenetic silencing of the genes through DNA methylation (Figure 1A). We also analyzed HCT116 cells in which the DNA methyltransferase genes *DNMT1* and *DNMT3B* were genetically disrupted (DKO2 cells), thereby abrogating DNA methylation (21). Those cells showed substantially greater expression of *IGFBP7* mRNA than the parental HCT116 cells (Figure 1A). In contrast to the cancer cells, *IGFBP7* was well expressed in normal colonic mucosa from a healthy individual (Figure 1A).

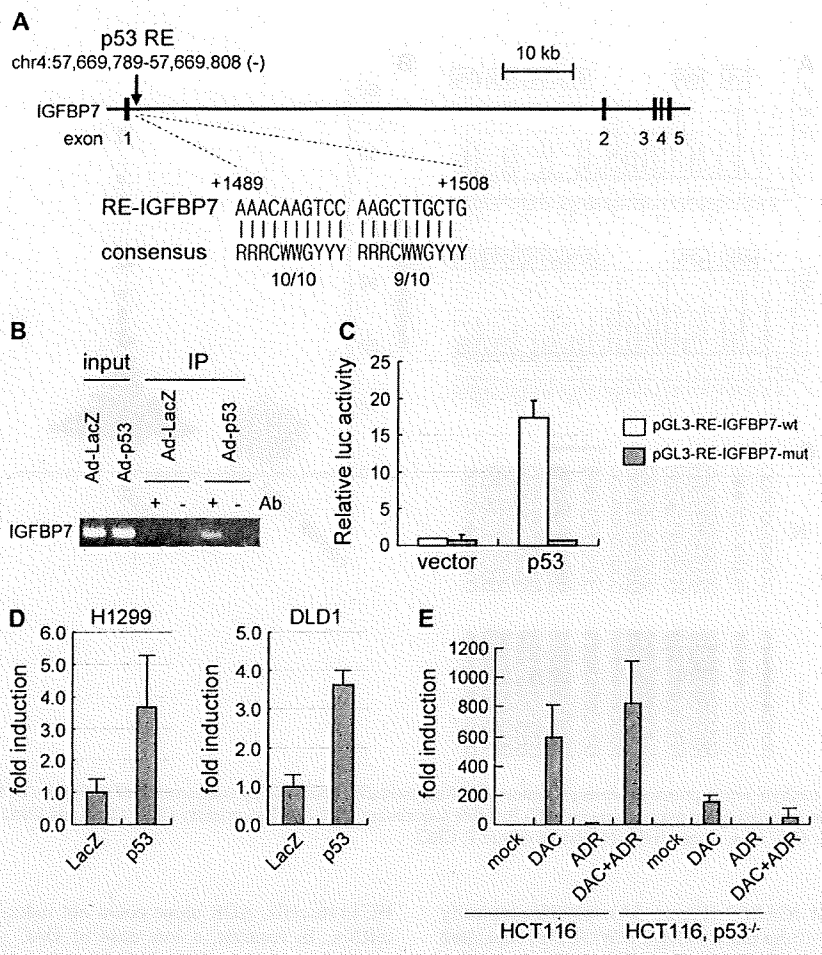


**Fig. 3.** Transcriptional activation of *IGFBP7* by p53. **(A)** In silico identification of p53REs. The structure of *IGFBP7* within the genome is shown. The putative p53RE in *IGFBP7* is shown as RE-*IGFBP7*. The nucleotide sequences of conserved p53REs are shown below (consensus). **(B)** ChIP analysis of *IGFBP7* p53RE. ChIP analysis was carried out using DLD-1 cells transfected with Ad-LacZ or Ad-p53, after which the chromatin was immunoprecipitated with anti-p53 antibody. The DNA was subjected to PCR using primers amplifying the region around RE-*IGFBP7*. **(C)** Luciferase assay for RE-*IGFBP7*. H1299 cells were cotransfected with empty vector or p53 plus pGL3-RE-*IGFBP7* or pGL3-RE-*IGFBP7*-mut. The relative luciferase activity was defined as the activity in the cells transfected with pGL3-RE-*IGFBP7* divided by the activity in cells transfected with pGL3-RE-*IGFBP7*-mut. **(D)** Induction of *IGFBP7* by p53. **(E)** Restoration of p53-induced *IGFBP7* expression by DAC.

When we then used TaqMan real-time reverse transcriptase–PCR to determine the relative levels of *IGFBP7* expression in the same samples, the results were consistent with those summarized above (Figure 1B), which strongly suggests that, in CRC, *IGFBP7* is a frequent target of epigenetic silencing through DNA methylation.

*Analysis of IGFBP7 methylation in CRC cell lines*

Because *IGFBP7* contains a CpG island in the region around its transcription start site, we next carried out MSP analysis using the primers illustrated in Figure 2A. We found that *IGFBP7* is completely or strongly methylated in the six CRC cell lines (Colo320, DLD1, HCT116, HT29, RKO and SW48) in which *IGFBP7* is silenced or downregulated (Figure 2B). In addition, detectable but relatively weak methylation was also found in cell lines (CaCO2, LoVo and DKO2) in which *IGFBP7* was expressed and in normal colonic mucosa (Figure 2B).

We verified the MSP results in selected samples using bisulfite sequencing, which revealed that the CpG island of *IGFBP7* is extensively methylated in CRC cell lines in which methylation was detected by MSP (Figure 2C). We also carried out a quantitative analysis of the methylation of six CpG sites located at the core of the CpG island using primers designed for bisulfite pyrosequencing (Figure 2D and E). The results confirmed the presence of high levels of methylation in cells in which *IGFBP7* expression was silenced or downregulated (DLD1, HCT116, HT29, RKO and SW48). In contrast, methylation levels were lower in cell lines in which *IGFBP7* was expressed (CaCO2, LoVo and SW480). DKO2 cells and normal colonic mucosa also showed low levels of *IGFBP7* methylation. In summary, we observed an inverse correlation between DNA methylation and *IGFBP7* expression in CRC cells.

To confirm that the CpG island is the promoter driving *IGFBP7* expression, we carried out ChIP–PCR to assess trimethylation of H3K4, which is reportedly a marker of active promoters (28). In both DAC-treated HCT116 cells and DKO2 cells, we observed significant enrichment of trimethylated H3K4 in the CpG island. In contrast, very little trimethylated H3K4 was detected in untreated HCT116 cells (Figure 2F).

*Identification of IGFBP7 as a target gene of p53*

We previously used a comparative genomic approach in which p53RE was employed as probe to identify novel p53 target genes (14). Using the same in silico analysis in the present study, we found a putative

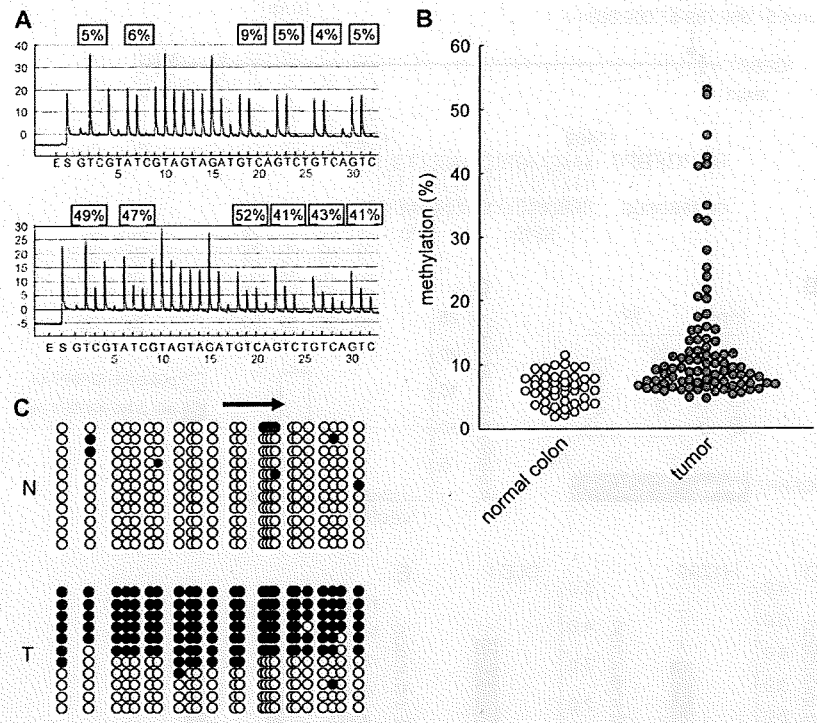


**Fig. 4.** Analysis of *IGFBP7* methylation in primary colorectal tumors. (**A**) Representative results of pyrosequencing of *IGFBP7*. (**B**) Diagram summarizing the levels of *IGFBP7* methylation detected using pyrosequencing. (**C**) Bisulfite sequencing of *IGFBP7* in primary CRC: Open and filled circles represent unmethylated and methylated CpG sites, respectively: N, normal colon; T, CRC.

p53RE within intron 1 of *IGFBP7* (Figure 3A). p53REs typically consist of two copies of a 10 bp motif (RRRCWWGYYY) separated by 0–12 bp. The putative p53RE for *IGFBP7* (RE-*IGFBP7*) contains a mismatch at a non-critical position within the 20 bp consensus p53-binding sequence (Figure 3A). To determine whether, in fact, p53 directly binds to RE-*IGFBP7*, we carried out ChIP assays using DLD1 cells infected with Ad-p53. After immunoprecipitating DNA–protein complexes from the cross-linked extracts of Ad-p53-infected and control cells using an anti-p53 antibody, we used PCR amplification to measure the abundance of candidate p53REs within the immunoprecipitated complexes. Subsequent ChIP assays confirmed that p53 did indeed bind to DNA fragments containing RE-*IGFBP7* (Figure 3B). To then determine whether p53 can transactivate gene expression via RE-*IGFBP7*, we carried out promoter reporter assays using a luciferase vector containing the wild-type RE-*IGFBP7* sequence upstream of the basal SV40 promoter (pGL3-RE-*IGFBP7*-wt) and a control reporter containing an unresponsive mutated RE-*IGFBP7* sequence (pGL3-RE-*IGFBP7*-mut). H1299 cells, which are null for p53 (29), were transiently cotransfected with one of the reporter plasmids along with a p53 expression vector or an empty vector. In contrast to pGL3-RE-*IGFBP7*-mut, luciferase activity from pGL3-RE-*IGFBP7*-wt was significantly upregulated when cotransfected with a p53 (Figure 3C).

To investigate the effect of p53 on endogenous induction of *IGFBP7*, we assessed expression of *IGFBP7* mRNA in cell lines infected with Ad-p53. Real-time PCR showed that exogenous p53 induced expression of *IGFBP7* mRNA in both H1299 (p53 null, ref. 29) and DLD1 cells (p53 mutant, ref. 30) (Figure 3D). To then assess the role of endogenous p53 in the expression of *IGFBP7*, we treated HCT116 cells with ADR, an agent known to damage DNA and induce endogenous p53 expression, with or without DAC. In a previous study, we showed that ADR, but not DAC, activated p53 and that typical p53 target genes were significantly induced by ADR alone (14,31). However, because *IGFBP7* is methylated and silenced in HCT116 cells, ADR alone could not induce expression of *IGFBP7* mRNA. In contrast, a low dose of DAC (0.1 μM) did induce its expression, and we observed further upregulation *IGFBP7* transcription upon addition of ADR (Figure 3E). When we treated *p53*$^{-/-}$ HCT116 cells with the same low dose of DAC, the induction was quite weak, and no synergistic upregulation was seen upon addition of ADR (Figure 3E).

To determine the extent to which responsiveness to p53 is affected by methylation in the region around the p53REs, we assessed the methylation status of CpG sites in the vicinity of the p53REs. We found that the region around p53REs was methylated regardless of gene expression. Moreover, this region was also methylated in normal tissues, suggesting that methylation of p53REs does not affect the binding of p53 (supplementary Figure 2 is available at *Carcinogenesis* Online). Taken together, these observations support the idea that *IGFBP7* is a direct target of p53, and its induction can be blocked by DNA hypermethylation.

### *Growth suppressive effect of IGFBP7*

To test whether *IGFBP7* suppresses CRC cell growth, we cloned the full-length *IGFBP7* cDNA into pcDNA3.1 vector, after which we transfected HCT116 cells with the resultant pcDNA3.1His-IGFBP7 vector and verified secretion of the expressed IGFBP7 protein into the conditioned medium (supplementary Figure 1A is available at *Carcinogenesis* Online). We then tested the transfectants in colony formation assays and found that overexpression of IGFBP7 markedly suppressed colony formation (supplementary Figure 1B and C is available at *Carcinogenesis* Online).

### *Correlation between IGFBP7 methylation and other epigenetic/genetic alterations in CRC and adenoma*

We next analyzed the methylation of the *IGFBP7* CpG island in a panel of tumor specimens from CRC patients. Because MSP

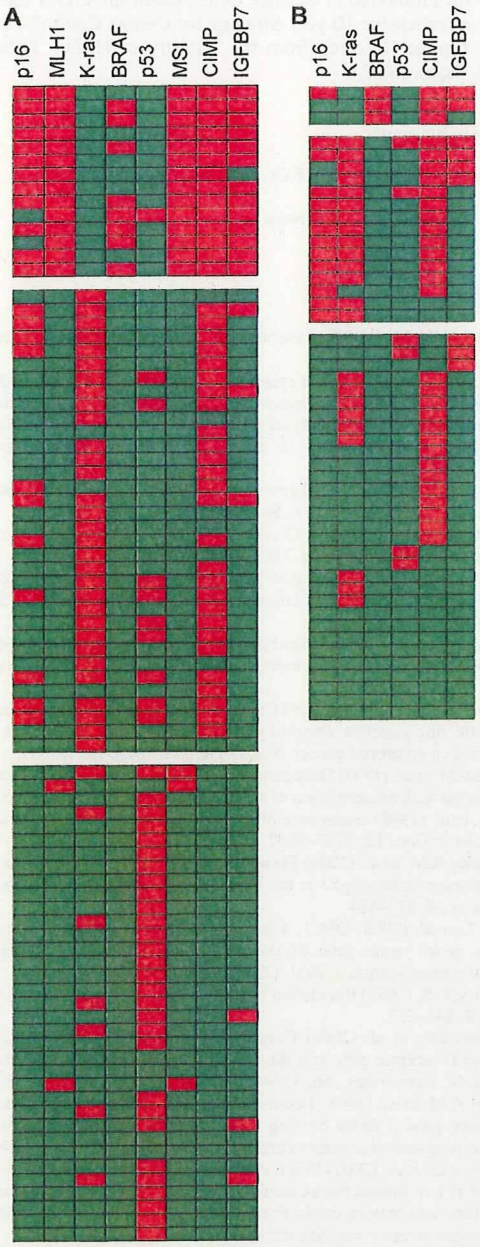


**Fig. 5.** Epigenetic and genetic alterations in CRCs (**A**) and colorectal adenomas (**B**). K-means clustering analysis based on epigenetic and genetic alterations. Each column represents the separate gene locus shown on the top. Each row is a primary CRC or adenoma: red rectangles, methylated/mutated tumors; green rectangles, unmethylated/wild-type tumors. Fifteen percent methylation was used as the cutoff criterion for methylation of *IGFBP7*.

revealed a low level of *IGFBP7* methylation in normal colonic mucosa, we carried out bisulfite pyrosequencing to quantitatively analyze *IGFBP7* methylation (Figure 4A). As summarized in Figure 4B, levels of *IGFBP7* methylation were significantly higher in primary tumors than in normal colonic tissue ($P < 0.001$). We confirmed these results with bisulfite sequencing in selected specimens. In normal colonic tissue, the vast majority of the CpG island was unmethylated (Figure 4C). On the other hand, tumor tissue in which elevated methylation was detected showed a mixture of entirely and partially

**Table I.** Correlation between methylation of IGFBP7 and other epigenetic and genetic alterations

| | | IGFBP7 methylation | | |
|---|---|---|---|---|
| | | Mean values | SD | *P* |
| Age | | $R = 0.117$ | | 0.292 |
| Sex | F (25) | 14.3 | 13.2 | 0.563 |
| | M (58) | 12.8 | 9.4 | |
| p16 | Unmethylated (60) | 10.2 | 6.1 | 0.002 |
| | Methylated (23) | 21.4 | 15.1 | |
| hMLH1 | Unmethylated (67) | 9.7 | 4.5 | <0.001 |
| | Methylated (16) | 28.4 | 15.0 | |
| K-ras | Wild-type (45) | 16.7 | 13.1 | 0.001 |
| | Mutated (38) | 9.2 | 3.7 | |
| BRAF | Wild-type (75) | 11.0 | 7.3 | 0.001 |
| | Mutated (8) | 35.2 | 12.5 | |
| p53 | Wild-type (44) | 16.4 | 13.1 | 0.003 |
| | Mutated (39) | 9.8 | 5.0 | |
| MSI | Stable (66) | 9.7 | 4.5 | <0.001 |
| | Unstable (17) | 27.2 | 15.3 | |
| CIMP | Absent (42) | 9.6 | 4.8 | 0.002 |
| | Present (41) | 17.0 | 13.4 | |

methylated alleles and unmethylated alleles, probably reflecting contamination of the sample by normal cells (Figure 5C).

Finally, we examined the correlation between *IGFBP7* methylation and other genetic and epigenetic alterations in CRCs (Figure 5A, Table I). We found that there are significant correlations between levels of *IGFBP7* methylation and methylation of *p16* ($P < 0.001$) and *hMLH1* ($P < 0.001$), mutation of *BRAF* ($P < 0.001$), CIMP ($P = 0.002$) and microsatellite instability ($P < 0.001$). Levels of *IGFBP7* methylation were inversely correlated with mutation of *K-ras* ($P = 0.001$) and *p53* ($P = 0.014$). Of 49 colorectal adenomas, nine (18%) showed *IGFBP7* methylation and three (6%) showed *BRAF* mutation, while none showed *hMLH1* methylation or microsatellite instability, indicating that inactivation of *IGFBP7* is an early event in colorectal tumorigenesis (Figure 5B).

## Discussion

A subset of CRCs show methylation of multiple CpG islands, indicating that these tumors have CIMP (5). CRCs with CIMP are closely associated with microsatellite instability through methylation of *hMLH1* (5) and frequently show *BRAF* mutations (8), which indicates that these tumors arise via distinct pathways that differ from classical multistep tumorigenesis (6). In the present study, we found that methylation of *IGFBP7* is strongly associated with *BRAF* mutation and the presence of CIMP. Moreover, the earlier finding that *BRAF* mutations are common in hyperplastic polyps and serrated adenomas suggests CRCs with CIMP/*IGFBP7* methylation arise via the serrated pathway (32). It is also known that Ras-mediated epigenetic silencing of effectors, including DNMT1, plays a key role in cellular transformation (33) and that DNMT1 is a downstream target of the Ras-signaling pathway (34). This suggests that *BRAF* activation may be involved in the CIMP phenotype through activation of the DNA methylation machinery. Because the colorectal adenomas examined in this study were not serrated adenomas, further study will be necessary to determine the incidence of *IGFBP7* methylation among serrated adenomas.

It remains unclear why CIMP is associated with *BRAF* mutation. Mutations leading to *BRAF* activation are found in several types of human tumors. Substituting a glutamic acid for a valine at position 600 (BRAFV600E) substantially increases BRAF's protein kinase activity, leading to constitutive extracellular signal-regulated kinase signaling (35,36). However, activation of BRAFV600E does not fully transform primary human cells, indicating that additional cooperative events are required for tumorigenesis (37). Indeed, expression of BRAFV600E induces senescence in cultured primary human

melanocytes (37). And although BRAF mutations are frequently seen in colorectal hyperplastic polyps, these tumors undergo senescence (38). It has therefore been speculated that genes involved in the induction of senescence by BRAF are altered during the progression of tumors. In addition, IGFBP7 was recently shown to play an important role in Ras-mediated senescence (19). Our results thus suggest that CRCs with CIMP may escape senescence by both activating oncogenic signaling (e.g. *BRAF* mutations) and inactivating regulators of senescence (e.g. *IGFBP7* methylation).

The regulatory mechanisms controlling *IGFBP7* expression are not fully understood. p53 is a transcription factor that activates expression of genes involved in cell cycle checkpoints, apoptosis and DNA repair (39). Although CRCs with CIMP show only a low frequency of p53 mutations, the function of p53 may nonetheless be impaired in these tumors due to epigenetic inactivation of target genes, including *IGFBP* family members such as *IGFBP7* and *IGFBP3* (40). Consistent with that idea, several targets of p53 are known to be silenced by DNA methylation (20,41,42). In the present study, we found that *IGFBP7* is not expressed in HCT116 cells but that expression could be restored by treating the cells with DAC. Moreover, Ad-p53 acts synergistically with DAC to further upregulate *IGFBP7* expression. These findings suggest that combining a DNA methyltransferase inhibitor with drugs that induce p53-dependent growth inhibition may be a useful approach to treating CRC. In fact, Lin *et al.* (43) recently reported that reactivation of IGFBP7 using DAC inhibits CRC cell growth.

Weak methylation of *IGFBP7* was even detected in DKO2 cells. Although DKO2 cells lack both DNMT1 and DNMT3B, this cell line does express a different DNA methyltransferase, DNMT3A, which may maintain the observed methylation. Alternatively, residual activity of truncated DNMT1 may be sufficient to maintain the low level of *IGFBP7* methylation seen in DKO2 cells (44). In addition, expression of *IGFBP7* was not fully restored by DAC treatment in HT29 and RKO cells (Figure 1B), which suggests that other cofactors involved in induction of *IGFBP7* also may be impaired in these cell lines.

The molecular mechanism by which IGFBP7 contributes to tumor suppression is not fully understood, though IGFBP7 has been shown to suppress cell growth and induce apoptosis (45,46). In lung and prostate cancers, for example, IGFBP7 induces apoptosis by upregulating expression of Caspase-3 (47,48). On the other hand, knocking down IGFBP7 had no effect on cell growth *in vitro*, though IGFBP7 did suppress anchorage-independent and *in vivo* cell growth (49), suggesting that the effects of IGFBP7 on cell growth vary depending upon the cell type. IGFBP7 is a cell adhesion factor that promotes cell adhesion by binding to cell surface heparin sulfate proteoglycans (50,51). Because CRCs showing expression of IGFBP7 do not grow *in vivo*, Sato *et al.* (49) proposed that although IGFBP7 is involved in cell adhesion, it suppresses anchorage-dependent cell growth *in vivo*. Further study will be necessary to clarify the mechanism by which IGFBP7 modulates growth signaling pathways to suppress the growth of cancer cells.

In summary, we found that *IGFBP7* is a direct target of p53, indicating that IGFBP7 is a mediator of p53-dependent growth suppression. DAC and Ad-p53 acted synergistically to induce *IGFBP7* expression in CRC cells where it was otherwise silenced by methylation. We also found that *IGFBP7* methylation is associated with the *BRAF* mutations, the absence of p53 mutations and the presence of CIMP in CRCs. Thus, epigenetic inactivation of *IGFBP7* appears to be a potentially useful molecular target for the diagnosis and treatment of CRCs with CIMP.

## Supplementary material

Supplementary Figures 1 and 2 and Table 1 can be found at http://carcin.oxfordjournals.org/

## Funding

Grants-in-Aid for Scientific Research on Priority Areas from the Ministry of Education, Culture, Sports, Science and Technology (K.I., T.T. and M.T.); Grants-in-Aid for Scientific Research (S) from Japan Society for Promotion of Science (K.I.); Grant-in-Aid for the Third-term Comprehensive 10 year Strategy for Cancer Control; Grant-in-Aid for Cancer Research from the Ministry of Health, Labor, and Welfare, Japan (M.T.).

## Acknowledgements

The authors thank Dr William F.Goldman for editing the manuscript.

*Conflict of Interest Statement:* None declared.

## References

1. Kinzler,K.W. *et al.* (1996) Lessons from hereditary colorectal cancer. *Cell*, **87**, 159–170.
2. Jones,P.A. *et al.* (2007) The epigenomics of cancer. *Cell*, **128**, 683–692.
3. Kanai,Y. *et al.* (2007) Alterations of DNA methylation associated with abnormalities of DNA methyltransferases in human cancers during transition from a precancerous to a malignant state. *Carcinogenesis*, **28**, 2434–2442.
4. Ushijima,T. *et al.* (2005) Aberrant methylations in cancer cells: where do they come from? *Cancer Sci.*, **96**, 206–211.
5. Toyota,M. *et al.* (1999) CpG island methylator phenotype in colorectal cancer. *Proc. Natl Acad. Sci. USA*, **96**, 8681–8686.
6. Shen,L. *et al.* (2007) Integrated genetic and epigenetic analysis identifies three different subclasses of colon cancer. *Proc. Natl Acad. Sci. USA*, **104**, 18654–18659.
7. Toyota,M. *et al.* (2000) Distinct genetic profiles in colorectal tumors with or without the CpG island methylator phenotype. *Proc. Natl Acad. Sci. USA*, **97**, 710–715.
8. Weisenberger,D.J. *et al.* (2006) CpG island methylator phenotype underlies sporadic microsatellite instability and is tightly associated with BRAF mutation in colorectal cancer. *Nat. Genet.*, **38**, 787–793.
9. Serrano,M. *et al.* (1997) Oncogenic ras provokes premature cell senescence associated with accumulation of p53 and p16INK4a. *Cell*, **88**, 593–602.
10. Zhu,J. *et al.* (1998) Senescence of human fibroblasts induced by oncogenic Raf. *Genes Dev.*, **12**, 2997–3007.
11. Kortlever,R.M. *et al.* (2006) Plasminogen activator inhibitor-1 is a critical downstream target of p53 in the induction of replicative senescence. *Nat. Cell Biol.*, **8**, 877–884.
12. Qian,Y. *et al.* (2008) DEC1, a basic helix-loop-helix transcription factor and a novel target gene of the p53 family, mediates p53-dependent premature senescence. *J. Biol. Chem.*, **283**, 2896–2905.
13. el-Deiry,W.S. (1998) Regulation of p53 downstream genes. *Semin. Cancer Biol.*, **8**, 345–357.
14. Maruyama,R. *et al.* (2006) Comparative genome analysis identifies the vitamin D receptor gene as a direct target of p53-mediated transcriptional activation. *Cancer Res.*, **66**, 4574–4583.
15. Burger,A.M. *et al.* (1998) Down-regulation of T1A12/mac25, a novel insulin-like growth factor binding protein related gene, is associated with disease progression in breast carcinomas. *Oncogene*, **16**, 2459–2467.
16. Landberg,G. *et al.* (2001) Downregulation of the potential suppressor gene IGFBP-rP1 in human breast cancer is associated with inactivation of the retinoblastoma protein, cyclin E overexpression and increased proliferation in estrogen receptor negative tumors. *Oncogene*, **20**, 3497–3505.
17. Lin,J. *et al.* (2007) Methylation patterns of IGFBP7 in colon cancer cell lines are associated with levels of gene expression. *J. Pathol.*, **212**, 83–90.
18. Yamashita,S. *et al.* (2006) Chemical genomic screening for methylation-silenced genes in gastric cancer cell lines using 5-aza-2′-deoxycytidine treatment and oligonucleotide microarray. *Cancer Sci.*, **97**, 64–71.
19. Wajapeyee,N. *et al.* (2008) Oncogenic BRAF induces senescence and apoptosis through pathways mediated by the secreted protein IGFBP7. *Cell*, **132**, 363–374.
20. Toyota,M. *et al.* (2008) Epigenetic silencing of microRNA-34b/c and B-cell translocation gene 4 is associated with CpG island methylation in colorectal cancer. *Cancer Res.*, **68**, 4123–4132.
21. Rhee,I. *et al.* (2002) DNMT1 and DNMT3b cooperate to silence genes in human cancer cells. *Nature*, **416**, 552–556.
22. Bunz,F. *et al.* (1998) Requirement for p53 and p21 to sustain G2 arrest after DNA damage. *Science*, **282**, 1497–1501.
23. Herman,J.G. *et al.* (1996) Methylation-specific PCR: a novel PCR assay for methylation status of CpG islands. *Proc. Natl Acad. Sci. USA*, **93**, 9821–9826.

24. Sasaki,Y. *et al.* (2003) Identification of the interleukin 4 receptor alpha gene as a direct target for p73. *Cancer Res.*, **63**, 8145–8152.
25. Nojima,M. *et al.* (2007) Frequent epigenetic inactivation of SFRP genes and constitutive activation of Wnt signaling in gastric cancer. *Oncogene*, **26**, 4699–4713.
26. Akino,K. *et al.* (2005) The Ras effector RASSF2 is a novel tumor-suppressor gene in human colorectal cancer. *Gastroenterology*, **129**, 156–169.
27. Eisen,M.B. *et al.* (1998) Cluster analysis and display of genome-wide expression patterns. *Proc. Natl Acad. Sci. USA*, **95**, 14863–14868.
28. Barski,A. *et al.* (2007) High-resolution profiling of histone methylations in the human genome. *Cell*, **129**, 823–837.
29. Chen,J.Y. *et al.* (1993) Heterogeneity of transcriptional activity of mutant p53 proteins and p53 DNA target sequences. *Oncogene*, **8**, 2159–2166.
30. Yu,J. *et al.* (1999) Identification and classification of p53-regulated genes. *Proc. Natl Acad. Sci. USA*, **96**, 14517–14522.
31. Adachi,K. *et al.* (2004) Identification of SCN3B as a novel p53-inducible proapoptotic gene. *Oncogene*, **23**, 7791–7798.
32. Minoo,P. *et al.* (2007) Prognostic significance of mammalian sterile20-like kinase 1 in colorectal cancer. *Mod. Pathol.*, **20**, 331–338.
33. Gazin,C. *et al.* (2007) An elaborate pathway required for Ras-mediated epigenetic silencing. *Nature*, **449**, 1073–1077.
34. Bakin,A.V. *et al.* (1999) Role of DNA 5-methylcytosine transferase in cell transformation by fos. *Science*, **283**, 387–390.
35. Davies,H. *et al.* (2002) Mutations of the BRAF gene in human cancer. *Nature*, **417**, 949–954.
36. Rajagopalan,H. *et al.* (2002) Tumorigenesis: RAF/RAS oncogenes and mismatch-repair status. *Nature*, **418**, 934.
37. Michaloglou,C. *et al.* (2005) BRAFE600-associated senescence-like cell cycle arrest of human naevi. *Nature*, **436**, 720–724.
38. Minoo,P. *et al.* (2006) Senescence and serration: a new twist to an old tale. *J. Pathol.*, **210**, 137–140.
39. Riley,T. *et al.* (2008) Transcriptional control of human p53-regulated genes. *Nat. Rev. Mol. Cell Biol.*, **9**, 402–412.
40. Buckbinder,L. *et al.* (1995) Induction of the growth inhibitor IGF-binding protein 3 by p53. *Nature*, **377**, 646–649.
41. Suzuki,H. *et al.* (2000) Inactivation of the 14-3-3 sigma gene is associated with 5′ CpG island hypermethylation in human cancers. *Cancer Res.*, **60**, 4353–4357.
42. Wales,M.M. *et al.* (1995) p53 activates expression of HIC-1, a new candidate tumour suppressor gene on 17p13.3. *Nat. Med.*, **1**, 570–577.
43. Lin,J. *et al.* (2008) Reactivation of IGFBP7 by DNA demethylation inhibits human colon cancer cell growth *in vitro*. *Cancer Biol. Ther.*, **7**, 1896–1900.
44. Egger,G. *et al.* (2006) Identification of DNMT1 (DNA methyltransferase 1) hypomorphs in somatic knockouts suggests an essential role for DNMT1 in cell survival. *Proc. Natl Acad. Sci. USA*, **103**, 14080–14085.
45. Sprenger,C.C. *et al.* (2002) Over-expression of insulin-like growth factor binding protein-related protein-1(IGFBP-rP1/mac25) in the M12 prostate cancer cell line alters tumor growth by a delay in G1 and cyclin A associated apoptosis. *Oncogene*, **21**, 140–147.
46. Wilson,H.M. *et al.* (2002) Insulin-like growth factor binding protein-related protein 1 inhibits proliferation of MCF-7 breast cancer cells via a senescence-like mechanism. *Cell Growth Differ.*, **13**, 205–213.
47. Chen,Y. *et al.* (2007) Insulin-like growth factor binding protein-related protein 1 (IGFBP-rP1) has potential tumour-suppressive activity in human lung cancer. *J. Pathol.*, **211**, 431–438.
48. Mutaguchi,K. *et al.* (2003) Restoration of insulin-like growth factor binding protein-related protein 1 has a tumor-suppressive activity through induction of apoptosis in human prostate cancer. *Cancer Res.*, **63**, 7717–7723.
49. Sato,Y. *et al.* (2007) Strong suppression of tumor growth by insulin-like growth factor-binding protein-related protein 1/tumor-derived cell adhesion factor/mac25. *Cancer Sci.*, **98**, 1055–1063.
50. Akaogi,K. *et al.* (1994) Cell adhesion activity of a 30-kDa major secreted protein from human bladder carcinoma cells. *Biochem. Biophys. Res. Commun.*, **198**, 1046–1053.
51. Sato,J. *et al.* (1999) Identification of cell-binding site of angiomodulin (AGM/TAF/Mac25) that interacts with heparan sulfates on cell surface. *J. Cell. Biochem.*, **75**, 187–195.

*Received March 7, 2009; revised June 21, 2009; accepted July 17, 2009*

Cell Stem Cell
Brief Report

# *Rest* Promotes the Early Differentiation of Mouse ESCs but Is Not Required for Their Maintenance

Yasuhiro Yamada,[1,3,4,5,*] Hitomi Aoki,[2,5] Takahiro Kunisada,[2] and Akira Hara[1]
[1]Department of Tumor Pathology
[2]Department of Tissue and Organ Development, Regeneration, and Advanced Medical Science
Gifu University Graduate School of Medicine, Gifu, 501-1194, Japan
[3]Center for iPS Cell Research and Application (CiRA), Institute for Integrated Cell-Material Sciences, Kyoto University, Kyoto 606-8507, Japan
[4]PRESTO, Japan Science and Technology Agency, 4-1-8 Honcho Kawaguchi, Saitama, Japan
[5]These authors contributed equally to this work
*Correspondence: y-yamada@cira.kyoto-u.ac.jp
DOI 10.1016/j.stem.2009.12.003

The functional significance of *Rest* in the maintenance of ESC pluripotency remains controversial. We herein showed that *Rest* is not necessary for the maintenance of mouse ESCs, and instead suggested that the Rest transcriptional repressor connects to the Oct3/4-Sox2-Nanog core regulatory circuitry during early ESC differentiation.

The pluripotency of ESCs is maintained by coordinated expression of a core regulatory circuit of genes that includes Oct3/4, Sox2, and Nanog. Rest (also called Nrsf) is abundantly expressed in ESCs and is a target of the Oct3/4-Sox2-Nanog regulatory network. However, the functional significance of Rest in the maintenance of pluripotency remains controversial. We have generated *Rest* conditional knockout and *Rest*-inducible ESC lines. Conditional ablation of *Rest* showed that it is not required for maintenance of pluripotency, but it is involved in the suppression of self-renewal genes during early differentiation of ESCs. In addition, forced expression of *REST* in ESCs results in rapid differentiation. These results indicate that *Rest* is not necessary for the maintenance of mouse ESCs, and instead suggest that the Rest transcriptional repressor connects to the Oct3/4-Sox2-Nanog core regulatory circuitry during early ESC differentiation.

The transcriptional repressor Rest is a zinc finger protein that binds to a conserved 23 bp motif known as RE1 (repressor element 1, also called NRSE) in a number of genes encoding the fundamental neuronal traits (Chong et al., 1995; Schoenherr and Anderson, 1995). Rest is expressed throughout early development where it represses the expression of neural genes, such as *Syp* and *Syt4* (Schoenherr et al., 1996). Rest is also expressed in ESCs and it has also been shown to be one of target genes of the regulatory circuitry of the pluripotent state in ESCs (Johnson et al., 2008; Sun et al., 2005). However, the functional significance of Rest in the maintenance of pluripotency in ESCs still remains controversial (Buckley et al., 2009; Jørgensen et al., 2009a; Singh et al., 2008). A previous study with a heterozygous *Rest* ESC line combined with an siRNA knockdown indicated that Rest maintains pluripotency through the induction of self-renewal genes, such as *Oct3/4*, *Nanog*, and *Sox2* (Singh et al., 2008). In contrast, Jørgensen et al. generated a *Rest* null ESC line and reported that such *Rest* null ESCs revealed no substantial change in either the Oct3/4 protein levels or alkaline phosphatase activity in comparison to matched wild-type controls (Jørgensen et al., 2009a, 2009b).

In order to elucidate the role of *Rest* in the maintenance of pluripotency, we first generated an ESC line and mice that contained the conditional knockout alleles of *Rest*. The first *Rest* allele in the ESCs (V6.5) was replaced with the KO vector carrying the floxed last exon of *Rest*, which encodes the coRest binding site that is essential for the generation of the silencing complex (Andrés et al., 1999; Grimes et al., 2000), followed by *ires-Gfp* to monitor the transcription of the modified allele ($Rest^{3lox/+}$; Figure 1A). The transient expression of *Cre recombinase* generated a *Rest* floxed ESC line that lacks a drug selection cassette ($Rest^{2lox/+}$). Analyzing the GFP expression allowed us to confirm that *Rest* is expressed in ESCs (Figure 1B).

$Rest^{-/-}$ ESCs were next generated with the floxed *Rest* ESC line together with a plasmid expressing *Cre recombinase* (Figure 1A). After the excision of the floxed *Rest* gene by the transient transfection of *Cre* ($Rest^{+/-\ (1lox)}$), the second *Rest* allele was also replaced with the floxed allele ($Rest^{3lox/-}$). The transient transfection of *Cre* into $Rest^{3lox/-}$ ESCs resulted in the establishment of $Rest^{-/-}$ ESCs that were isogenic to the parental ESCs without any genetic modification except for the *Rest* alleles.

After the recombination of the *Rest* alleles, the lack of a *Rest* transcript in such $Rest^{-/-}$ ESCs was confirmed by a northern blot analysis (Figure 1B; Figure S1A available online). Consistent with the recombination, a FACS analysis revealed a lack of any GFP signal in the $Rest^{-/-}$ ESCs (Figure 1B). In addition, a western blot analysis revealed the lack of any Rest protein in such $Rest^{-/-}$ ESCs (Figure 1B). *Syt4* possesses RE1 and it is expressed while relying solely on dissociation of the Rest repressor complex from the RE1 site for maximal expression (Ballas et al., 2005). The expression of *Syt4* significantly increased in the $Rest^{-/-}$ ESCs, thus indicating that the Rest-targeted gene is derepressed in $Rest^{-/-}$ ESCs (Figure S1B).

Consistent with the findings by Jørgensen et al. (2009a, 2009b), the growth and morphology of the $Rest^{-/-}$ ESCs were indistinguishable from those of wild-type V6.5 ESCs under the self-renewal conditions (under the presence of LIF and MEF). Furthermore, when the expression of the pluripotent genes was compared, the expression of *Nanog*, *Oct3/4*, and *Sox2* in $Rest^{-/-}$ ESCs were not altered

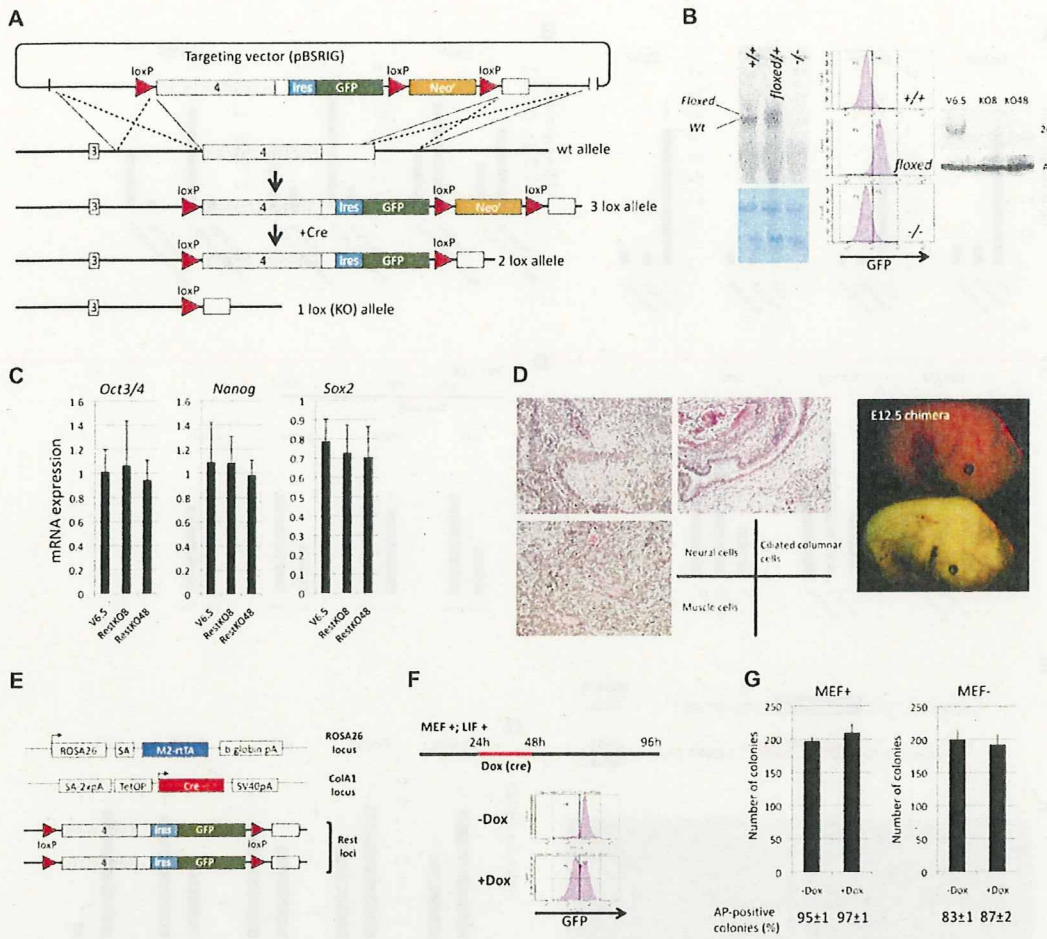


**Figure 1. *Rest* Is Not Required for the Maintenance of ESC Pluripotency**

(A) A schematic drawing of the *Rest*-conditional knockout vector and targeted *Rest* allele.

(B) A northern blot analysis reveals a lack of *Rest* transcripts. GFP fluorescence is observed to have disappeared in the $Rest^{-/-}$ ESCs. A western blot analysis shows the absence of any Rest protein in two independent knockout ESC lines, RestKO8 and RestKO48.

(C) Transcript levels of pluripotent genes in $Rest^{-/-}$ ESCs. No significant changes in the expression of *Oct3/4*, *Nanog*, and *Sox2* are detectable in the $Rest^{-/-}$ ESCs relative to the control ESCs. Transcript levels were normalized to *β-actin* levels. The data are presented as the average values with SD of six independent samples.

(D) $Rest^{-/-}$ teratomas differentiate into three different germ layers, including neural cells, ciliated columnar cells, and muscle cells. E12.5 chimeric mice were generated by injecting $Rest^{-/-}$ ESCs into blastocysts.

(E) A schematic drawing of the conditional *Rest* knockout ESC line containing doxycycline-inducible *Cre* alleles.

(F) An experimental protocol. Conditional *Rest* knockout ESCs were treated with doxycycline (2 μg/ml) for 24 hr starting at 24 hr and then were harvested at 96 hr after the passage. A FACS analysis revealed the presence of GFP-negative cells, thus indicating the occurrence of *Rest* ablation at 96 hr after passage.

(G) The conditional deletion of the *Rest* gene does not suppress the development of alkaline phosphatase (AP)-positive ESC colonies under the presence or absence of feeder cells. *Rest*-floxed *Cre*-inducible ESCs were exposed to doxycycline and then were fixed after 3 days of exposure. The total number of colonies and the percent positivity for AP are indicated. The data are presented as the mean ± SD of three independent 35 mm wells.

in comparison to those in the control ESCs (Figure 1C). To further examine the pluripotency of $Rest^{-/-}$ ESCs, $Rest^{-/-}$ ESCs were next injected into the subcutaneous tissue of nude mice. $Rest^{-/-}$ ESCs could generate teratomas with evidence of differentiation into three different germ layers (Figure 1D). To fully evaluate the differentiation ability of the $Rest^{-/-}$ ESCs, GFP-labeled $Rest^{-/-}$ ESCs were injected into blastocysts followed by transplantation into the uteri of pseudo-pregnant mice to generate chimeric embryos (Yamada et al., 2004). Eventually, this generated E12.5 chimeric mice with the widespread contribution of GFP-positive cells into the three germ layers (Figure 1D; Figure S1C).

In order to rule out the possibility that the adaptive responses, which occurred as a result of multiple cell passages, reduced the requirement of Rest-mediated maintenance of ESCs, the initial response of the gene expression was examined after the conditional ablation of the *Rest* genes. For this purpose, an ESC line was derived from transgenic embryo that harbors a doxycycline-inducible *Cre* transgene together with *Rest*-floxed alleles (Figure 1E; *Rest 2lox/2lox*;

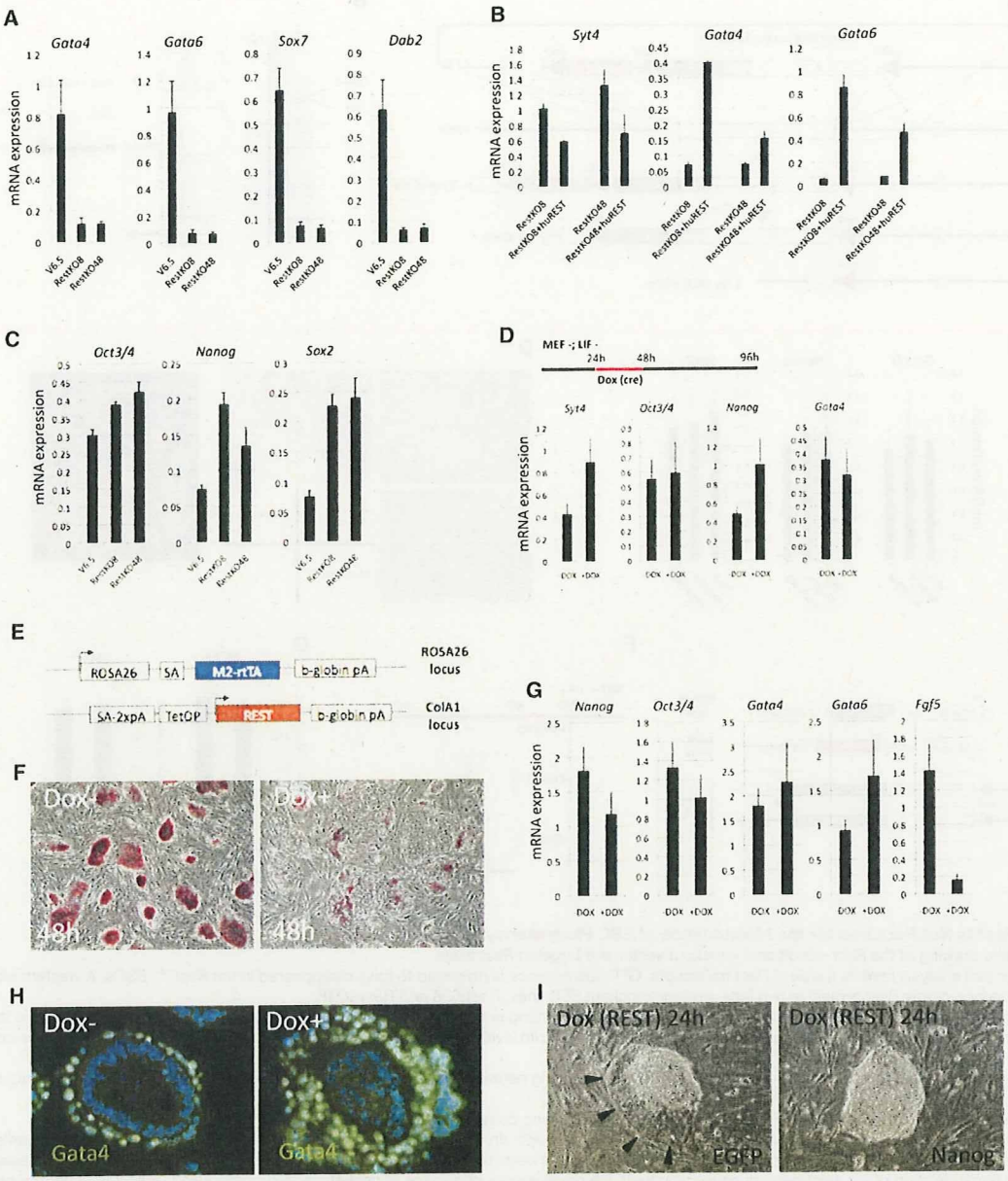


**Figure 2. *Rest* Promotes Primitive Endoderm Differentiation in ESCs**

(A) Under confluent culture conditions, the expression of *Gata4* and *Gata6* were significantly lower in the $Rest^{-/-}$ ESCs in comparison to the control isogenic ESCs (V6.5). The expression of *Sox7* and *Dab2*, which are both markers for the primitive endoderm, are suppressed in $Rest^{-/-}$ ESCs. Transcript levels were normalized to *β-actin* levels. The data are presented as the average values with SD of six independent samples.

(B) The exogenous expression of *REST* rescued the suppression of *Gata4* and *Gata6* in $Rest^{-/-}$ ESCs. Mean ± SD of three independent samples.

(C) The expression of pluripotent genes in the embryoid body (EB) cells. The expression of *Occt3/4*, *Nanog*, and *Sox2* are upregulated in $Rest^{-/-}$ EB cells relative to the control EB cells. The data are presented as the mean ± SD of six independent samples.

(D) Conditional *Rest* knockout ESCs were cultured under differentiation culture conditions and treated with doxycycline (2 μg/ml) for 24 hr starting at 24 hr. The cells were harvested at 96 hr after the passage. The expression of *Syt4*, *Oct3/4*, *Nanog*, and *Gata4* after the conditional deletion of *Rest* under the differentiation culture condition. Note that the expression of *Nanog* and *Syt4*, but not of *Oct3/4*, were upregulated in the doxycycline-treated cells. The data are presented as the mean ± SD of six independent samples.

(E) A schematic drawing of the doxycycline-inducible *REST* ESC line.

(F) 48 hr of the induction of *REST* causes the ESC differentiation into epithelium-like colonies with a decreased AP activity.

(G) The forced expression of *REST* in ESCs leads to decreased expression of *Nanog*, *Oct3/4*, and *Fgf5*, whereas it results in increased expression of *Gata6*. The data are presented as the mean ± SD of six independent samples.

(H) In vitro differentiation of *REST*-inducible ESCs into EBs under the absence or presence of doxycycline. The exogenous *REST* expression results in an increased number of Gata4-positive cells at the periphery of EBs.